# Size-Resolved Aerosol Composition near Rocky Mountain National Park

A THESIS
Presented to
The Environmental Program
Colorado College

In Partial Fulfillment
of the Requirements for the Degree
Bachelor of Arts in Environmental Science

By
Rachel Sussman
May 2016

Approved By:

Lynne Gratz, Ph.D.
Assistant Professor, Environmental Program

Howard Drossman, Ph.D.
Professor, Environmental Program

# Table of Contents

## Abstract

Increasing our understanding of aerosol properties is important because of their potential impacts on visibility, human health, and sensitive ecosystems. The Rocky Mountain Airborne Nitrogen and Sulfur (RoMANS) study was conducted in 2006 to identify the sources, transport, and speciation of atmospheric gases and aerosols throughout Colorado that influence Rocky Mountain National Park (RMNP). As one component of this study, Micro-Orifice Uniform Deposition Impactor (MOUDI) samples were collected at two sites in the vicinity of RMNP. Samples were taken over a time span of 48 hours each during a period of 36 days in the spring (March-April) and summer (July-August). The samples were analyzed by ion chromatography to determine the concentrations of $NH_4^+$, $Na^+$, $Ca^{2+}$, $K^+$, $Mg^{2+}$, $Cl^-$, $NO_2^-$, $NO_3^-$, $SO_4^{2-}$, and $C_2O_4^{2-}$ in either ten or twelve different size bins from >18 μm to <0.18 μm.

The diameter of nitrate has important implications for nitrogen deposition in RMNP as larger particles have a higher deposition velocity. In the spring, nitrate was observed to be mainly in the accumulation mode while in the summer it was primarily in the coarse mode. Ammonium and sulfate were the dominant species in the accumulation mode and on several days the sulfate was sufficient to completely neutralize ammonium. However, there were a substantial number of days where the addition of nitrate and oxalate to the ammonium neutralization was not enough to account for complete neutralization. The excess ammonium suggests that other organic acids may be an important component of the aerosol in the region.

There is a dearth of research on the size distribution and secondary formation pathways of organic acids, such as aerosol oxalate, which might be contributing to haze and acting as cloud condensation nuclei. The size distribution of oxalate was found to peak in the accumulation mode, specifically between 0.32 and 0.56 µm. We examined three potential contributors to oxalate concentrations: biomass burning, in-cloud processes, and gas-phase photo-oxidation. All three were found to be likely emission and formation mechanisms, but it is unclear which pathway is dominant.

## Introduction

The atmosphere is composed of molecules in the gas, liquid, and solid phases. These molecules interact with each other to form new species – sometimes in different phases – in ways that are dependent on the conditions of the environment in which they exist. Aerosols are solid particles in the atmosphere that can range from nanometers ($10^{-9}$ m) to micrometers ($10^{-6}$ m) in diameter. They can be formed by homogenous (gas-phase) or heterogeneous (between phases) reactions or they can be directly emitted from anthropogenic or biogenic sources. The secondary formation pathways of many aerosols are poorly understood, as are the impacts of aerosols on human and environmental health. Increasing evidence is being presented that aerosols can be significant to both humans and the environment: small aerosols (below approximately 2.5 μm in diameter - $PM_{2.5}$) can pass into human lungs, where they can lead to respiratory illnesses, heart problems, and early mortality, while both large and small aerosols can impact the environment in various ways (Lightly et al. 2009). Determining how and under what conditions these particles are formed is essential to designing and implementing effective mitigation and response policies.

Aerosols are also taking a front stage in the discussion surrounding climate change. Anthropogenic aerosol loading has exponentially increased the concentrations of various aerosols (IPCC 2013). These aerosols can have direct and indirect effects on climate: the particles themselves can scatter or absorb solar radiation, and they can also impact cloud formation and dynamics, the effects of which are poorly understood in relation to climate (IPPC 2013). Together, these properties of aerosols might have a significant effect on the Earth's energy balance, but the uncertainties surrounding aerosols make it difficult to estimate the total net anthropogenic effect on climate (IPPC 2013; Figure 1).

One of the most significant indicators of an aerosol's effects on its surroundings is its size. There are two main classes of particle size: fine and coarse. Figure 2 shows the modes, sources, and deposition pathways of aerosols of various sizes. Particles below approximately 1.8 μm in diameter are in the fine mode, while particles larger than 1.8 μm are in the coarse mode (Seinfeld & Pandis 1998). Within the fine range is the accumulation mode (between about 0.1 and 1.8 μm) and the Aitken nuclei mode (between 0.01 and 0.1 μm). The size range of particles determines their methods of formation, transport, and deposition, and thus their function in the environment. Coarse mode particles tend to be mechanically generated from sources such as dust, sea spray, and volcanoes (Seinfeld & Pandis 2006). They deposit quickly from the atmosphere through sedimentation (settling). Accumulation mode particles are formed through chemical reactions. As the name suggests, these particles accumulate in the atmosphere and have long residence times because they are large enough not to coagulate and small enough not to settle gravitationally. They are removed from the atmosphere through wet deposition. Aerosols in the accumulation mode are the primary culprits of haze because they are so long-lived and because so many particles can gather together and scatter sunlight (Duan et al. 2006). They also are expected to have greater climate impacts because their size range is closer to the wavelengths of visible light, and therefore interact with solar radiation more than larger particles (Kanakidou et al. 2005). Nucleation mode aerosols form through condensation of hot vapor and are short-lived because they rapidly coagulate into accumulation mode particles. The majority of particles exist in the Aitkin mode, but the majority of particle mass is in the coarse mode (Willeke & Whitby 1975). A typical size distribution of particle concentration has two main peaks: coarse mode and accumulation mode.

Although there can be some variation if there are multiple generation pathways, many of the commonly measured ions have expected size distributions (Figure 3). Sulfate, ammonium, and nitrate are all chemically generated, and are thus present in the accumulation mode (Wall et al. 1988). Nitrate and sulfate can also be present in the coarse mode if nitric acid and sulfuric acid react with mechanically generated calcium carbonate in sea spray and dust (Zhuang et al. 1999). These sources are composed of calcium, sodium, and chloride, which are dominant in the coarse mode (Wall et al. 1998).

Because of the long-lasting and multifaceted human and environmental impacts of fine-mode particles, scientists are focused on understanding their precursors, sources, formation mechanisms, and deposition pathways. Of particular importance is organic material, which can comprise as much as 90% of total fine aerosol mass in tropical forested regions and up to 50% at continental mid-latitudes (Kanakidou et al. 2005). Water-soluble organic compounds (WSOC) are major constituents of the organic material, either as primary organic aerosols (POA) that are directly emitted, or as secondary organic aerosols (SOA; Kavouras et al. 1998). SOA can be formed either through the homogenous gas-phase oxidation of volatile organic compounds (VOCs), the products of which condense into aerosols, or through heterogeneous, in-cloud oxidation, in which gaseous species are drawn into cloud droplets, then remain as aerosols when the water evaporates (Kanakidou et al. 2005).

One of the most notable indirect impacts organic aerosols can have on climate is their interaction with cloud droplets. The  ability of aerosols to attract and absorb water is called hygroscopicity, which is usually expressed as the ratio of the particle humidified diameter to its dry particle diameter at a specific relative humidity (Kanakidou et al. 2005). Particles that are hygroscopic can attract and absorb water in the atmosphere, acting as cloud condensation nuclei (CCN). If CCN did not exist, clouds would only be able to form at unrealistically high relative humidity of several hundred percent (Hänel 1976). With the presence of hygroscopic atmospheric aerosols, however, clouds can form at equilibrium saturation (Hänel 1976). Because of the high reflectivity of cloud droplets, clouds have the potential to counteract the warming effects of greenhouse gases (Cruz & Pandis 1997). In order to fully comprehend climate dynamics, scientists need to understand the mechanisms and aerosols involved in the formation of clouds, and the formation pathways of those aerosols. Until recently, however, the hygroscopic properties of organic aerosols and their potential role in cloud condensation had remained uninvestigated. Considering the abundance of organics in the atmosphere, this neglect represented a major lapse in the understanding of CCN. Studies have since shown that organic aerosols can, in fact, act as CCN, which increases the proportion of particles that can be activated for cloud formation and decreases the activation diameter of the overall aerosol population (Cruz & Pandis 1997).

Haze is a type of urban pollution caused by anthropogenic and biogenic aerosol emission. In many regions of the world, the drastic increase in haze with growing populations and urban areas has led to multinational emission mitigation agreements and action plans. In the national parks in the United States, haze is one of the most worrisome environmental problems. Visibility has decreased from 140 miles to 35-90 miles in western parks and from 90 miles to 15-25 miles in eastern parks (EPA 2015a). There are two types of haze: wet and dry. Dry haze obscures visibility by scattering and absorbing incoming solar radiation, which increases the aerosol optical thickness (AOT; Kaufman et al. 2002; EPA 2015a). Fewer wavelengths of light reach the eye, so we perceive fewer colors and have lower visual ranges (EPA 2015a). This phenomenon is exacerbated when water condenses onto hygroscopic aerosols, creating wet haze (Levin et al. 2009). Traditionally, only inorganic aerosols were investigated with respect to visibility, but as evidence of the hygroscopicity of organic aerosols arose, so did research on the contribution of WSOCs to haze. Jiang et al. (2011) estimates that some WSOCs can cause as much haze and loss of visibility as water-soluble inorganic compounds.

Fully understanding WSOCs is crucial to accurately accounting for the environmental impacts of aerosols. One way of furthering our knowledge of WSOCs is by using a representative species to estimate the behavior and impacts of the entire group. One candidate for this representative compound is oxalic acid. Oxalic acid is a WSOC with the chemical formula $H_2C_2O_4$; its conjugate base is oxalate ($C_2O_4^{2-}$; Figure 4). It is the most abundant dicarboxylic acid and WSOC of the tropospheric aerosols in both rural and urban environments (Jiang et al. 2011; Yu et al. 2005). Therefore, it is a cloud condensation nucleus that might be changing the radiative forcing of other aerosols and is a significant contributor to haze (Jiang et al. 2011). It lies at the end of the oxidation chain of volatile organic compounds, and is the smallest dicarboxylic acid (Yu et al. 2005). Its precursors are thought to be compounds such as glyoxylic acid, glycolic acid, glyoaldehyds, and glyoxal (Yu et al. 2005; Figure 5).

Like many organic aerosols, the sources and formation mechanisms of aerosol oxalate are still topics for discussion. The primary sources of oxalate are emissions from fossil fuel combustion (which most studies agree contributes very little due to low correlations between oxalate and other vehicular emissions) and biomass burning (Yu et al. 2005; Jiang et al. 2011; Zhou et al. 2015). Dust and sea spray can also be sources, though not in the fine mode (Jiang et al. 2011). However, these sources alone are not enough to account for total aerosol oxalate concentrations; a significant portion must be coming from secondary formation pathways. As with other SOA, the most likely secondary pathways are homogenous and heterogeneous oxidation. Homogenous gas-phase oxidation involving a hydroxyl radical has been proven in smog chamber experiments (Seinfeld & Pandis 1998; Kalberer et al. 2000). Others have suggested that oxalic acid is being drawn into cloud droplets, where aqueous-phase oxidation creates aerosol oxalate.

Yu et al. (2005) proposed in-cloud processes as a dominant formation mechanism for oxalate. At several sites throughout Asia, high correlations were found between aerosol oxalate and sulfate, which is predominantly formed by in-cloud processing. Both species are present in the droplet mode (0.52-1.0 μm in diameter), both were found in larger concentrations inside and above clouds than below, and they have different precursors and emission sources so the correlation cannot be attributed to these factors. Therefore, Yu et al. (2005) concluded that the common variable must be a dominant secondary formation pathway common to both species: in-cloud processing.

This in-cloud pathway has been generally accepted as a likely secondary formation pathway for aerosol oxalate. However, other studies dispute the relative contribution of this mechanism. Martinelango et al. (2007) found negative correlations between relative humidity and oxalate concentrations, which would be unlikely if it was being formed in precipitation. The high correlations between oxalate and nitric acid, formaldehyde, and ozone (all of which have photochemical production pathways) indicate gas-phase photo-oxidation (Martinelango et al. 2007). Jiang et al. (2007) pointed to the high correlation between fine-mode nitrate, which is produced via gas-phase photo-oxidation, and oxalate as evidence that this pathway could be significant. Other studies used Positive Matrix Factorization (PMF), a type of factor analysis that creates “profiles” for the sources of a specified particle, to estimate the relative contributions of different sources and formation pathways (EPA 2015, 2). Zhou et al. (2015), using PMF, attributed 37% of oxalate production to biomass burning, 33% to gas-phase oxidation, and only 16% to aqueous processes. These studies and others suggest that an in-cloud pathway might not be the dominant formation mechanism, but the results are still inconclusive and vary widely with location, time of year, and collection methodology.

In the spring and summer seasons of 2006, the National Park Service funded a state-wide investigation of aerosol sulfur and nitrogen in Colorado called the Rocky Mountain Airborne Nitrogen and Sulfur study (RoMANS). The study was implemented in response to concerns about aerosols in RMNP, which were thought to be negatively impacting the park’s sensitive high-elevation ecosystems and degrading visibility throughout the area. The goals of the study were to “1) Identify the overall mix of oxidized and reduced nitrogen in the air and precipitation on the east and west sides of the Continental Divide, 2) identify the relative contributions of nitrogen at Rocky Mountain National Park from emissions originating within the state of Colorado and outside the state, as well as relative contributions of in-state regions, and 3) identify the relative contributions of differing source types including mobile, agricultural, other area sources, and large and small point sources (NPS 2006).” In order to achieve these goals, various types of sampling missions were undertaken at sites throughout the state (Figure 6). The following study utilizes data from one of these 2006 RoMANS sampling missions in order to better understand the size distributions and concentrations of aerosols in Rocky Mountain National Park. It aims to establish the anions neutralizing ammonium and balancing the atmosphere, and contributes to the debate surrounding the secondary formation mechanisms of aerosol oxalate.

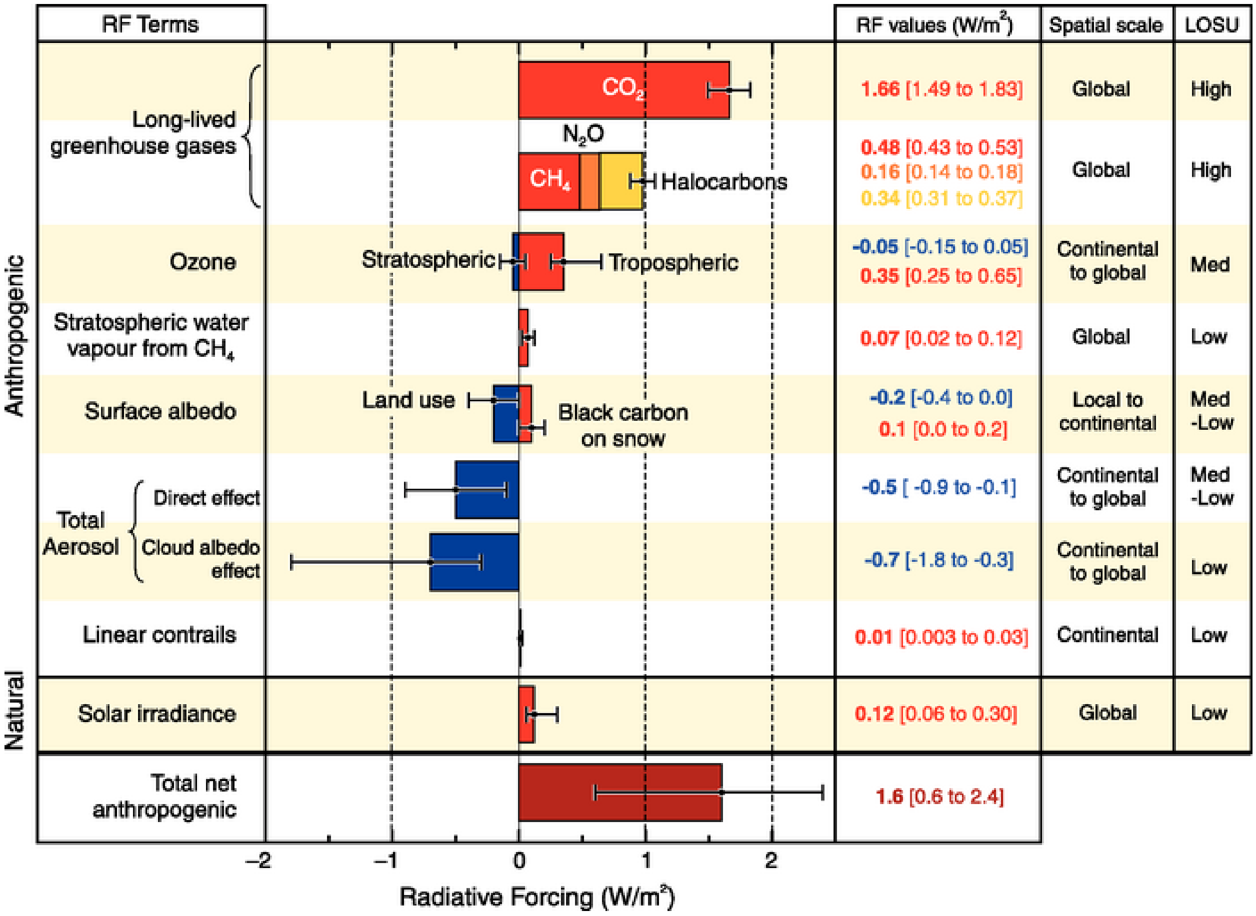

**Figure 1**: The radiative forcing balance of Earth. Aerosols are thought to have a negative effect on radiative forcing, but there are large uncertainties that obscure our understanding of the total net anthropogenic effect on climate (IPCC 2013).

**Figure 2**: Idealized schematic of the distribution of particle surface area of an atmospheric aerosol (Whitby & Cantrell 1976).

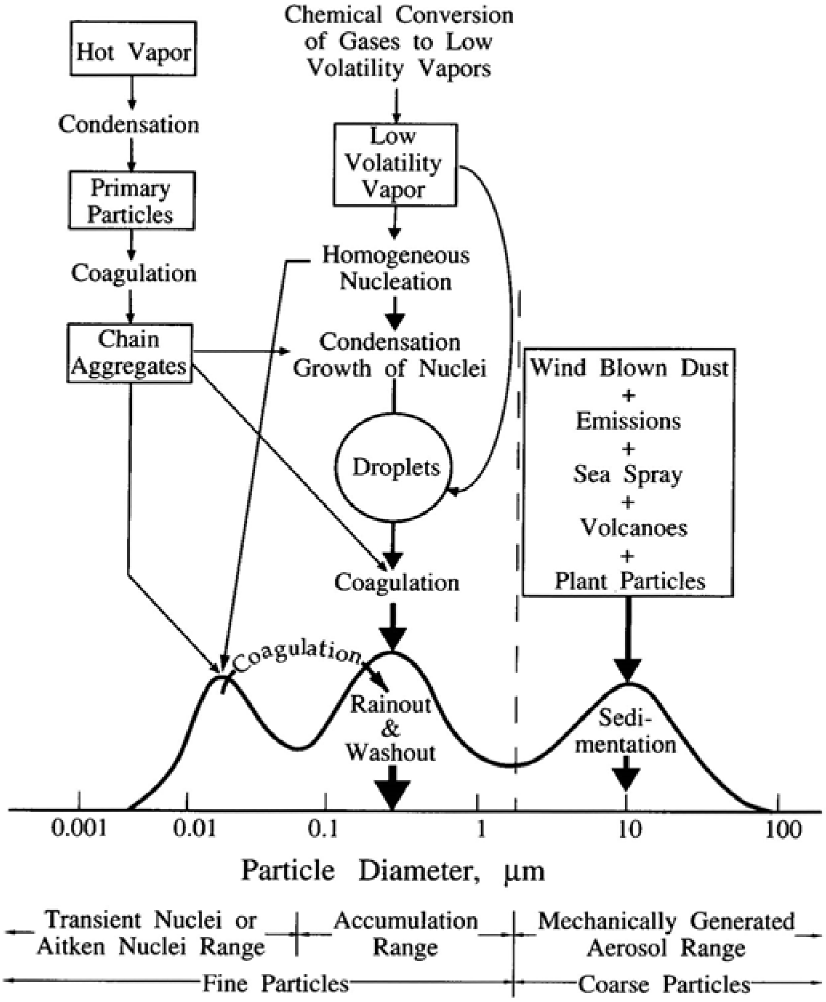

**Figure 3**: The size distribution of aerosol ammonium, nitrate, sulfate, hydrogen, sodium, and chloride in Claremont, CA (Wall et al. 1988).

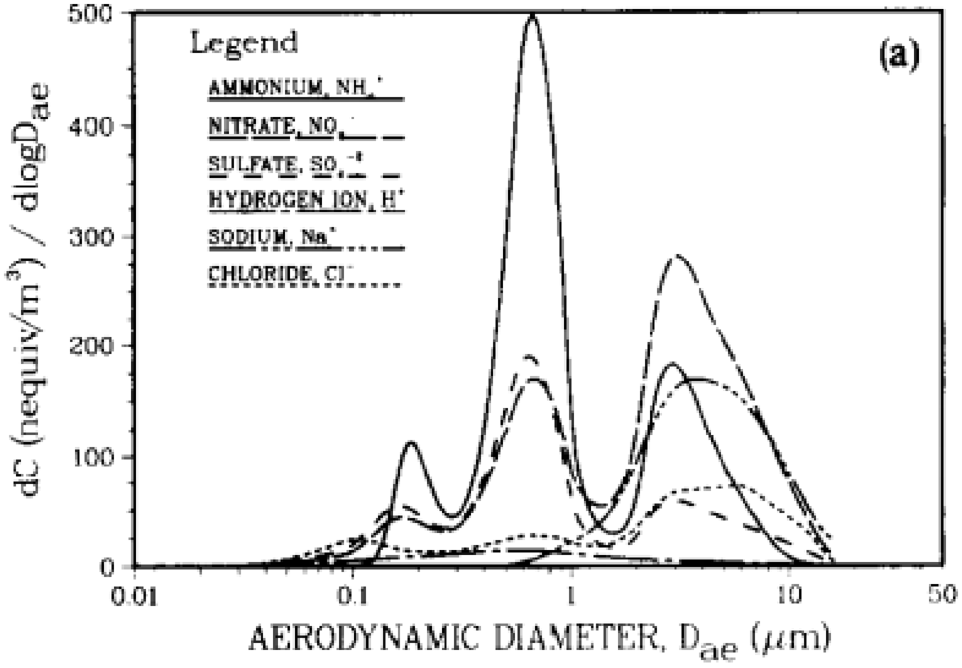

**Figure 4**: The chemical structure of a) oxalic acid and b) oxalate.

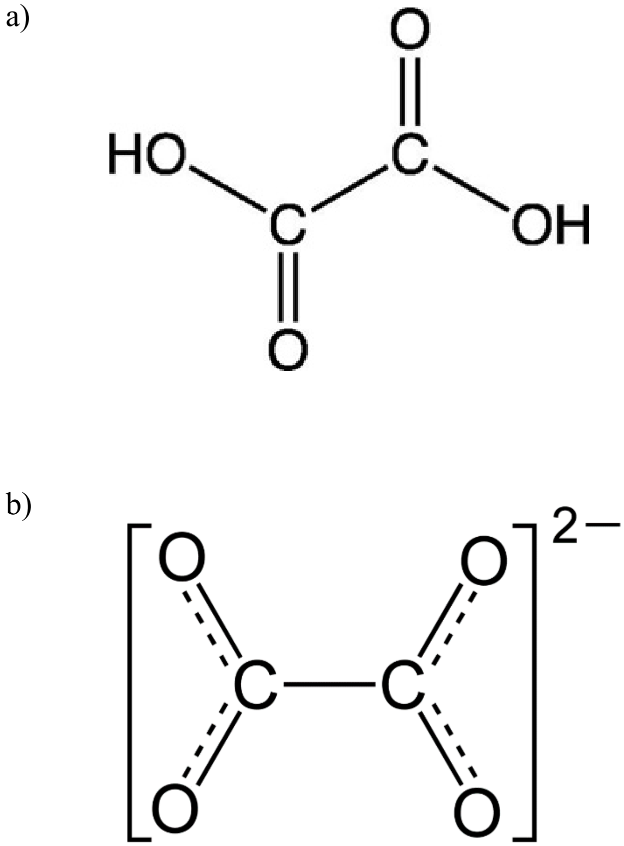

**Figure 5**: The oxidation chain of oxalic acid (adapted from Santos et al. 2009).

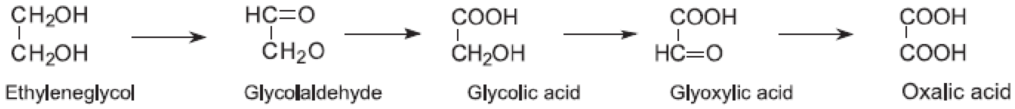

**Figure 6**: Map showing key measurement locations and sampling types during the RoMANS study (Beem et al. 2010).

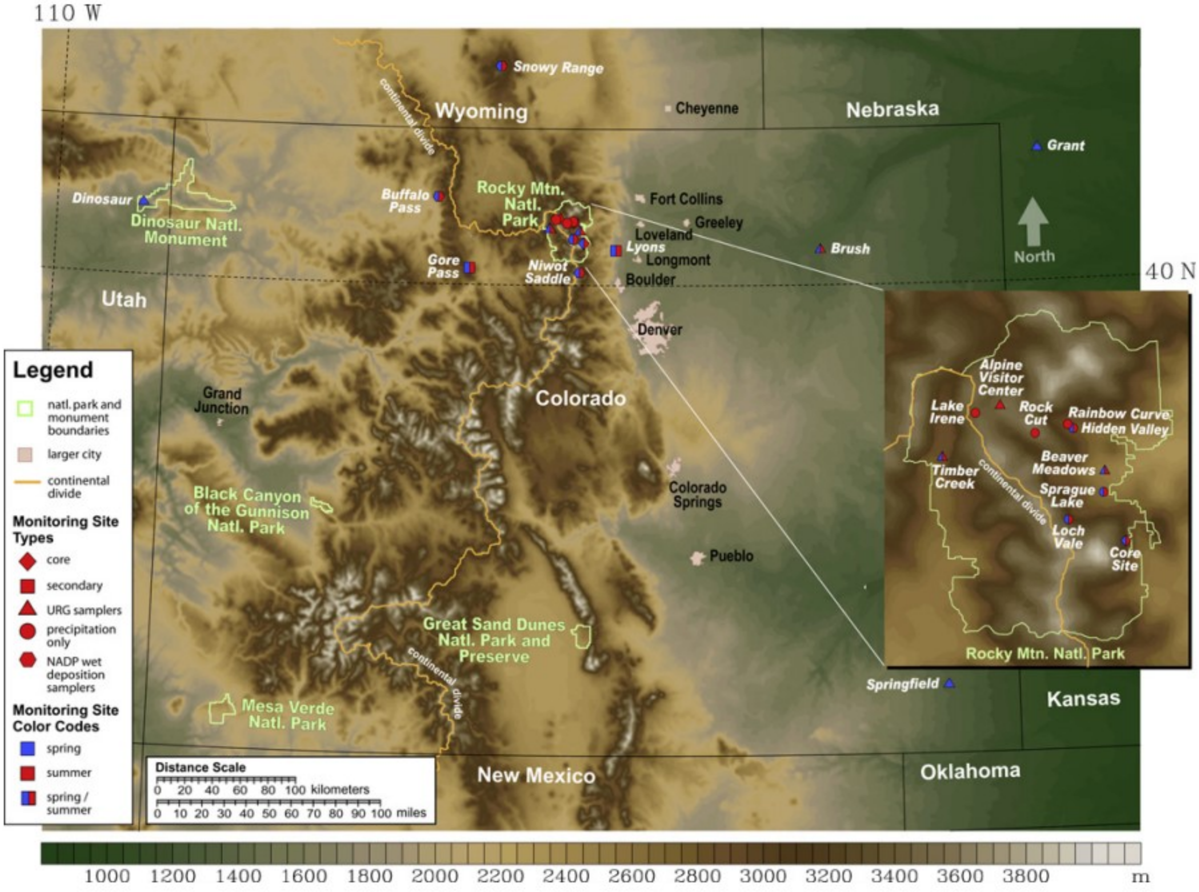

## Methods

### *Sites*

Data from two of the RoMANS sampling locations were used in this study (Figure 7). The first location, called the Main Site (MS), is within the national park (40.2783, -105.5457). At a relatively pristine location at the base of Longs Peak, this site has been used for many types of atmospheric monitoring within the park. There is very little foot and vehicular traffic moving through the area, so it provides a good baseline for ambient atmospheric conditions. It is at an elevation of 2743.2 m. The second site is the Lyons Site (LS; 40.2273, -105.2751). Lyons is situated in the urban corridor between Fort Collins and Boulder at an elevation of 1652.5 m. The city of Lyons has a population of about 2,000 people, is approximately 75 km north of Denver, and is 41 km southeast from the Main Site. Lyons itself is not heavily polluting, but it is downwind of larger urban areas and receives air pollution from them. It serves as the more polluted site when compared with the Main Site.

### *Field sampling*

Aerosol samples were taken using a Micro-Orifice Uniform Deposit Impactor (MOUDI). The MOUDI offers greater size resolution of atmospheric particles than traditional impactors. MOUDIs have a series of ten or twelve stages that are stacked directly on top of each other. Each stage has precisely cut holes that decrease in size from the top stage (M0) to the bottom stage (M9 or M11). The corresponding size ranges are shown for each MOUDI stage in Table 1. At each stage there is a filter on a collection plate. Air is pulled through the MOUDI by an attached air pump. As the air passes through each stage, some particles are collected by the impactor plate. However, only particles of a certain size hit each plate; smaller particles simply go around the plate and move on to the next stage (Hering & Marple 1986). The size of the aerosol that is collected at each stage is related to the size of the holes at each stage. When the holes decrease in size, the air is accelerated and particles have a harder time following the air stream moving around the plate (Hering & Marple 1986). By the time the air has moved to the bottom stage of the MOUDI, only the smallest aerosols remain. The final stage does not have a path around the collection plate, so all remaining particles are collected. Because the holes at every stage are cut so precisely, the size range of particles that impact at each plate is known.

Samples were taken over a 48-hour time period (filters were changed at 8:00 am every other day) at each site in both the spring and summer, following the method described in Lee et al. (2008). In the spring, samples were collected from March 25th until April 28th, and in the summer from July 6th until August 9th. The date, collection time, the initial and final volumes of the air pump, and the initial and final air pressure were recorded for each sampling period. The filters were put into labeled petri dishes and sealed. The Lyons samples were then transferred into test tubes and frozen at the CSU Fort Collins Atmospheric Science campus. The Main Site samples were frozen in the petri dishes. When these Main Site samples were thawed and transferred into test tubes nine years later, some of the particles stuck to the petri dishes, potentially skewing the aerosol concentrations. We realized the problem too late to rectify it, but because the Main Site blank samples were extracted the same way, the Method Detection Limits for that site were higher to reflect the variability between samples. Unfortunately, the Main

Site Spring samples were misplaced in the interim time between collection and analysis and thus they are not included in the present analysis.

### *Laboratory analysis*

The remaining samples were extracted in the summer of 2015. Filters were removed from the petri dishes and put into test tubes with 6 mL of deionized water. The test tubes were placed in an ultrasonic bath, which vibrates the test tubes at a high frequency to help particles dissolve from the filter into the water. The sonicated fluid was then transferred to another test tube. Some of the fluid was put into two ion chromatograph (IC) vials, and the rest was stored at CSU for potential future use. The samples were then run through the IC to determine the concentrations of anions and cations in each sample. The approximate times it takes for each type of ion to exit the column have been experimentally determined, so the peaks on the graph can be labeled accordingly (using DX standards to test standards made in the lab). Calibration standards of known concentration are run through the IC and the area under each standard peak is integrated to create a calibration curve, which is then applied to convert from the IC's units (μS) into micronormals (μN), the concentration of the charges of the ion. This allows for a side-by-side comparison of particles with different charges.

### *Data analysis*

The air concentration was calculated by multiplying the μN concentration with the extraction volume and dividing by the total volume of air that had been pumped through the MOUDI over the 48-hour sampling period, giving units of microequivalents. If there were notable differences in starting and ending air pressure, this was also accounted for using the following equation:

$$V_{air}(m^3) = (F_v - I_v) \times (1 - (\frac{(F_p - I_p)/2}{Pa}))$$

in which $F_v$ and $I_v$ are the final and initial dry gas readings, $F_p$ and $I_p$ are the final and initial pressures drop readings, and Pa is the ambient pressure (Skoog et al. 1995).

In order to account for instrumental error, the Method Detection Limits (MDLs) were calculated following the EPA's 40 CFR 136 Procedure (Skoog et al. 1995). MDLs are statistically-determined values that help to distinguish actual measurements from background concentrations, which we calculated from blanks that were taken alongside the actual measurements (EPA 2011). Measurements that are statistically significantly different from a blank at a 99% confidence level are "real." In order to determine the MDL for each of the species, the following formula from Skoog et al. (1995) was used:

$$MDL = (S_{pooled})\ (t_{n-1,\propto-1=\ 0.99})\ (\sqrt{\frac{\Sigma n + 1}{\Sigma n * 1}})$$

$S_{pooled}$= pooled standard deviation
n= number of samples in each data set
$t_{n-1,\alpha-1=0.99}$= the t-value at a 99% confidence level and a standard deviation estimate with n-1 degrees of freedom

$S_{pooled}$ is the pooled standard deviation for multiple independent groups in a study that are assumed to have a common standard deviation (Lipsey & Wilson 2001). All of our blanks were taken at different sites and times, but with the same instrument and under the same conditions.

$$S_{pooled} = \sqrt{\frac{\Sigma(X_i - X_1)^2}{\Sigma n - k}}$$

$X_i$= blank concentration (µN)
$X_1$= average blank concentration for a species in a data set in (µN)
n= number of samples in each data set
k= number of data sets

The MDLs of every ion were calculated by dividing by the average air volume of the study and subtracting from each measured value of the appropriate species. This concentration was then divided by the difference in the log of the upper and lower values of the size range of each stage. The final concentrations were in units of microequivalents per cubic meter per micrometer (μeq/m$^3$/μm). Like μN, μeq are normalized to charges. We mostly looked at the concentrations of particles below 2.5 μm ($PM_{2.5}$), but unfortunately, 2.5 μm falls in the middle of the 1.8-3.2 μm sampling range of the MOUDI. In order to estimate $PM_{2.5}$ concentrations and allow for cross-study comparisons, the concentrations of species in the size bins lower than 1.8 μm were added together and the sum was then added to one-half the 1.8-3.2 μm concentrations.

There are two main comparisons that can be made between data sets: between sites (Lyons Summer and Main Summer) and between seasons (Lyons Spring and Lyons Summer). Since the samples were collected under the same conditions and over the same times periods, paired t-tests between the specified pairs of data sets were run to test differences between sites and seasons.

HYSPLIT back trajectories were initially calculated over the 48-hour time periods in order to determine from where air masses were coming to help identify the sources of some of the ions. However, the position of the sites in and along the Rocky Mountains complicate this analysis: the valley-mountain circulation in addition to other, more typical, circulation patterns obscure the sources of many of the air masses (Beem et al. 2010). Another complicating factor is the variation in elevation between sites that is not captured in the traditional HYSPLIT. Thus, the back trajectories of the air were not particularly helpful or telling about aerosol sources and were not included in the following analysis.

**Figure 7**: A map of the two sites.

**Table 1**: The size ranges of particles captured at each MOUDI stage.

| Stage Number | Size Range (µm) | Stage Mid-Point (µm) |
|---|---|---|
| M0 | 18-50 | 34 |
| M1 | 10-18 | 14 |
| M2 | 5.6-10 | 7.8 |
| M3 | 3.2-5.6 | 4.4 |
| M4 | 1.8-3.2 | 2.5 |
| M5 | 1.0-1.8 | 1.4 |
| M6 | 0.56-1.0 | 0.78 |
| M7 | 0.32-0.56 | 0.44 |
| M8 | 0.18-0.32 | 0.25 |
| M9 | 0.1-0.18 | 0.14 |
| M10 | 0.056-0.1 | 0.078 |
| M11 | 0.00001-0.056 | 0.028005 |

## Data Overview

Aerosols tend to fall into two size modes: fine and coarse. To reflect this bimodal distribution, the data was separated into two groups- below and above 1.8 µm in diameter- and analyzed independently. Tables 2 and 3 summarize the results of the summary statistics computed for each ion species measured at the two sites for fine and coarse mode particles, respectively. In the fine mode, Lyons Spring had the highest average concentrations of sodium ($Na^+$), ammonium ($NH_4^+$) , magnesium ($Mg^{2+}$), calcium ($Ca^{2+}$), chloride ($Cl^-$), nitrate ($NO_3^-$), and sulfate ($SO_4^{2-}$). Lyons Summer had the highest means for potassium ($K^+$), nitrite ($NO_2^-$), and oxalate ($C_2O_4^{2-}$). In the coarse mode, Lyons Spring had the highest means for magnesium, calcium, chloride, and sulfate, while Lyons Spring had the highest averages for ammonium, sodium, potassium, nitrite, nitrate, and oxalate. Main Summer never had the highest mean for a species.

The Main Site likely tends towards lower means because it is a more pristine area than the Lyons site. It is within Rocky Mountain National Park, in a location with little direct anthropogenic impact (few cars or hikers; Figure 7). Thus, it probably lacks the precursors for the secondary formation of fine particles and is further removed from direct emission sources of coarse particles than the Lyons site.

The standard deviations of both the fine and coarse mode data sets (Tables 2 and 3) tend to be higher than the means. Only the Main Summer ammonium, magnesium, and sulfate have higher means than standard deviations. These high standard deviations indicate that there is a wide spread of ion concentrations between different sampling periods. Some 48-hour periods had relatively high aerosol concentrations, while others were near or at zero. This variation within each data set indicates that the mean is not the best descriptor of the data. Tables 2 and 3 also include the medians for each site and season. Because the median is less influenced by outliers, it is potentially a better representation of the data. For every species in every data set, the median was somewhat smaller than the mean. This implies that days with abnormally high concentrations are skewing the mean, and thus the median is probably a better descriptor of the data. Relatively high skewness values for most species support the idea that the median is a more appropriate summary statistic.

Paired t-tests were run between Lyons Summer and Main Summer to test differences in ion concentrations between sites, and between Lyons Spring and Lyons Summer to gauge differences between seasons. Table 4 shows the p-values for all ten species for the two comparisons for fine and coarse data, respectively. Fine mode particles had statistically significant differences (p-value<0.01) between the two sites for ammonium, potassium, calcium, nitrate, sulfate, and oxalate, and *not* for sodium, magnesium, chloride, and nitrite. The ions that were not statistically significantly different are related to sea spray, indicating that there are not noteworthy differences in the amounts of sea spray transported to the sites in the summer (not surprising considering how far Colorado is from any oceans), especially in the fine range where there are very low concentrations of these mechanically generated particles. In the coarse mode, all of the differences were statistically significant. The differences in concentrations of sea-spray ions in this size range are perhaps a result of seasonal variations in circulation patterns.

Table 4 also shows the p-values for the Lyons Spring to Summer comparison for the fine and coarse ranges. In the paired t-test for fine mode aerosols, all of the ions had p-values less than 0.01 except for ammonium, nitrite, and sulfate. In the coarse mode, the p-values for ammonium, potassium, magnesium, calcium, and oxalate are statistically significant, while those for sodium, chloride, nitrite, nitrate, and sulfate are not. Nitrite does not seem to vary in any notable way across the two variables. Ammonium and sulfate varied with site but not with season in both the fine and coarse mode. Aerosols associated with sea spray are concentrated in the coarse mode, where they tended to differ significantly between the Main and Lyons sites, but not between seasons.

One of the notable differences between the data sets is the amount and size of nitrate in the spring compared to the summer. Figure 8 shows the average size distribution for nitrogen in Lyons Spring, while Figure 9 displays the average size distributions for the two Summer sets. There are clear discrepancies between the absolute maximums and the dominant mode in the two seasons. Nitrate in Lyons Spring is dominant in the fine mode, while in the Summer sites it is dominant in the coarse mode. However, the maximum values of the average coarse mode nitrate for both Lyons seasons are very similar (2.83 $\mu eq/m^3/\ \mu m$ for Lyons Spring and 2.38 $\mu eq/m^3/\ \mu m$ for Lyons Summer); the difference between the two seasons is in the concentration of fine mode nitrate: 11.5 and 0.190 $\mu eq/m^3/\ \mu m$ for Lyons Spring and Summer, respectively.

The reason for this discrepancy comes from the formation pathways for aerosol nitrate. The abundance of coarse mode nitrate is from the pairing of gaseous nitric acid with coarse mode calcium carbonate from dust and sea spray in the following reaction (Allen et al. 2015):

$$\mathbf{2HNO_3 + CaCO_3 \rightarrow Ca(NO_3)_2}$$

This reaction is not temperature-dependent, so it occurs at similar rates in both seasons. However, the reaction that produces fine mode nitrate is temperature dependent:

$$\mathbf{HNO_3 + NH_3 \rightarrow NH_4NO_3}$$

Under the cooler spring temperatures, the reaction runs forward, producing aerosol ammonium nitrate, but in the hotter summer months, the reverse reaction dominates and more of the nitrate is present as gaseous nitric acid (Stelson & Seinfeld 1982).

**Table 2**: The means, medians, and standard deviations of the ten ions at Lyons Spring (LSp), Lyons Summer (LS), and Main Summer (MS) for the fine mode data (diameters <1.8µm).

| | **statistic** | **$Na^+$** | **$NH_4^+$** | **$K^+$** | **$Mg^{2+}$** | **$Ca^{2+}$** | **$Cl^-$** | **$NO_2^-$** | **$NO_3^-$** | **$SO_4^{2-}$** | **$C_2O_4^{2-}$** |
|---|---|---|---|---|---|---|---|---|---|---|---|
| **LSp** | $\bar{x}$ | 1.15 | 13.34 | 0.14 | 0.38 | 1.13 | 0.30 | 0.10 | 4.12 | 8.06 | 0.27 |
| | *median* | 0.19 | 2.60 | 0.04 | 0.16 | 0.71 | 0.07 | 0.00 | 0.33 | 3.49 | 0.03 |
| | $s$ | 3.23 | 29.53 | 0.20 | 0.62 | 1.19 | 0.58 | 0.18 | 11.87 | 12.51 | 0.42 |
| **LS** | $\bar{x}$ | 0.16 | 8.19 | 0.34 | 0.09 | 0.25 | 0.08 | 0.19 | 0.31 | 7.64 | 0.77 |
| | *median* | 0.01 | 3.88 | 0.14 | 0.04 | 0.00 | 0.00 | 0.00 | 0.18 | 4.32 | 0.45 |
| | $s$ | 0.33 | 11.84 | 0.58 | 0.11 | 0.55 | 0.21 | 0.47 | 0.47 | 9.86 | 0.98 |
| **MS** | $\bar{x}$ | 0.10 | 4.00 | 0.21 | 0.11 | 0.63 | 0.09 | 0.13 | 0.15 | 3.41 | 0.23 |
| | *median* | 0.00 | 3.06 | 0.11 | 0.11 | 0.32 | 0.00 | 0.00 | 0.08 | 2.51 | 0.14 |
| | $s$ | 0.42 | 3.59 | 0.36 | 0.07 | 0.71 | 0.35 | 0.25 | 0.23 | 3.07 | 0.34 |

**Table 3**: The means, medians, and standard deviations of the ten ions at Lyons Spring, Lyons Summer, and Main Summer for coarse mode data (diameters >1.8μm).

| | statistic | $Na^+$ | $NH_4^+$ | $K^+$ | $Mg^{2+}$ | $Ca^{2+}$ | $Cl^-$ | $NO_2^-$ | $NO_3^-$ | $SO_4^{2-}$ | $C_2O_4^{2-}$ |
|---|---|---|---|---|---|---|---|---|---|---|---|
| **LSp** | $\bar{x}$ | 0.43 | 0.23 | 0.14 | 1.48 | 5.48 | 0.33 | 0.12 | 1.29 | 0.62 | 0.05 |
| | *median* | 0.37 | 0.16 | 0.00 | 0.55 | 5.00 | 0.24 | 0.00 | 0.70 | 0.43 | 0.00 |
| | *s* | 0.34 | 0.23 | 0.23 | 2.30 | 3.54 | 0.33 | 0.22 | 1.83 | 0.62 | 0.13 |
| **LS** | $\bar{x}$ | 0.45 | 0.34 | 0.24 | 0.51 | 4.20 | 0.25 | 0.16 | 1.32 | 0.54 | 0.22 |
| | *median* | 0.20 | 0.27 | 0.18 | 0.45 | 3.71 | 0.05 | 0.00 | 1.07 | 0.50 | 0.27 |
| | *s* | 0.92 | 0.34 | 0.25 | 0.31 | 2.79 | 0.63 | 0.30 | 1.10 | 0.27 | 0.20 |
| **MS** | $\bar{x}$ | 0.08 | 0.11 | 0.06 | 0.19 | 1.33 | 0.04 | 0.06 | 0.33 | 0.14 | 0.02 |
| | *median* | 0.00 | 0.10 | 0.05 | 0.14 | 0.93 | 0.00 | 0.00 | 0.21 | 0.14 | 0.00 |
| | *s* | 0.20 | 0.11 | 0.06 | 0.14 | 1.19 | 0.12 | 0.16 | 0.30 | 0.12 | 0.06 |

**Table 4**: The p-values from a paired t-test for comparisons between sites and seasons for a) fine mode and b) coarse mode particles. P-values below 0.01 are considered statistically significant. P-values above 0.01 are bolded.

a)

| | **$Na^+$** | **$NH_4^+$** | **$K^+$** | **$Mg^{2+}$** | **$Ca^{2+}$** |
|---|---|---|---|---|---|
| **LS to MS** | **0.33** | <0.01 | <0.01 | **0.12** | <0.01 |
| **LSp to LS** | <0.01 | **0.08** | <0.01 | <0.01 | <0.01 |

| | **$Cl^-$** | **$NO_2^-$** | **$NO_3^-$** | **$SO_4^{2-}$** | **$C_2O_4^{2-}$** |
|---|---|---|---|---|---|
| **LS to MS** | **0.74** | **0.24** | <0.01 | <0.01 | <0.01 |
| **LSp to LS** | <0.01 | **0.09** | <0.01 | **0.72** | <0.01 |

b.

| | **$Na^+$** | **$NH_4^+$** | **$K^+$** | **$Mg^{2+}$** | **$Ca^{2+}$** |
|---|---|---|---|---|---|
| **LS to MS** | <0.01 | <0.01 | <0.01 | <0.01 | <0.01 |
| **LSp to LS** | **0.8** | <0.01 | <0.01 | <0.01 | <0.01 |

| | **$Cl^-$** | **$NO_2^-$** | **$NO_3^-$** | **$SO_4^{2-}$** | **$C_2O_4^{2-}$** |
|---|---|---|---|---|---|
| **LS to MS** | <0.01 | <0.01 | <0.01 | <0.01 | <0.01 |
| **LSp to LS** | **0.26** | **0.26** | **0.89** | **0.16** | <0.01 |

**Figure 8**: The average size distribution for nitrate in Lyons Spring. The concentration peaks in the fine mode.

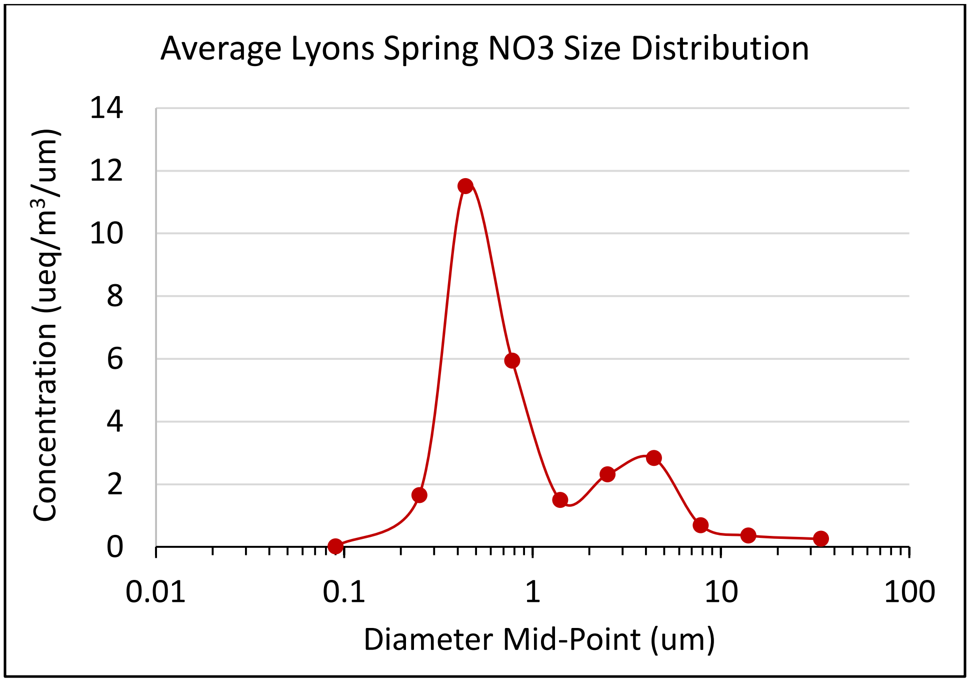

**Figure 9**: The average size distribution for nitrate in Lyons and Main Summer. The concentration peaks in the coarse mode.

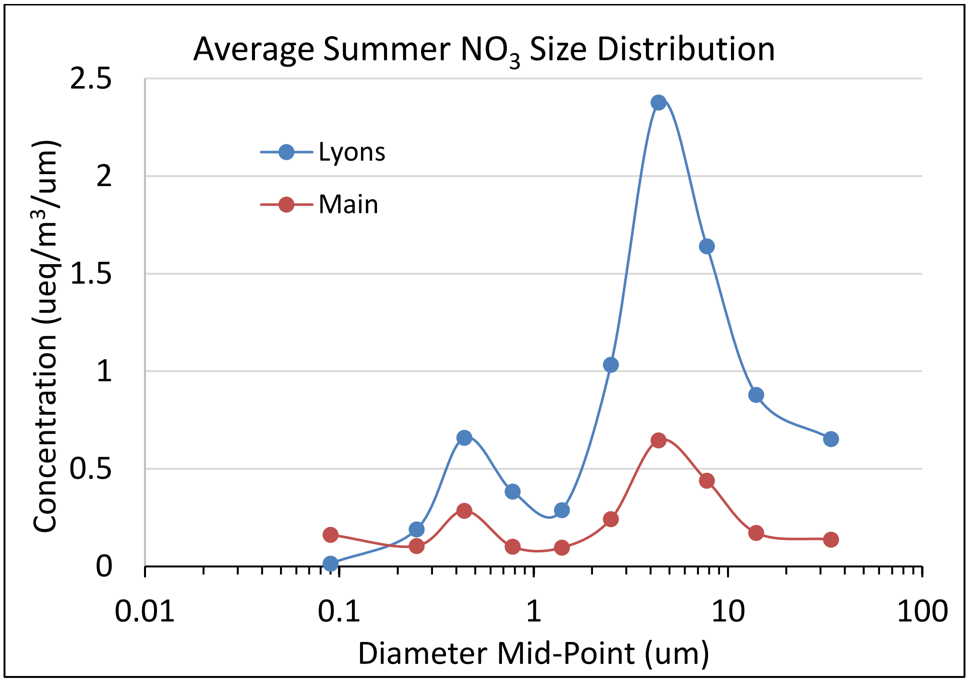

## Results and Discussion

### *Atmospheric Aerosol Neutralization*

The atmosphere is thought to be net neutral: the sum of the anion charges should equal the sum of the cation charges. By converting our data to units of microequivalents (rather than moles or mass), we were able to directly compare the anion and cation charges and determine whether the measured ions fully accounted for the charge balance of the atmosphere.

Figure 10 shows the average size distribution for a 48-hour period in Lyons Spring, Lyons Summer, and Main Summer. The graphs show the size distributions for the ten measured ions: ammonium, sodium, calcium, potassium, magnesium, chloride, nitrite, nitrate, sulfate, and oxalate. As noted in the previous section, the high standard deviations of each species relative to their means suggest that the averages might not be representative of the data sets as a whole because of the data's bimodal distribution. However, all of the individual graphs of each 48-hour time period had the same general shape and relative concentrations as the average graphs. All three data sets have a notable peak in concentration at the 0.32-0.56 µm size range, with a smaller peak in the 3.2 to 5.6 µm range. Because the vast majority of particles are present in 0.32-0.56 µm range, most of the neutralizing occurs here. Therefore, only this size range is examined.

Ammonium is clearly the most abundant ion in all three data sets. Its most likely source is from cattle urine and fertilizer from agricultural operations in eastern Colorado (Benedict et al. 2013). The other four cations are insignificant to the total cation concentration and thus we chose to disregard them to simplify the charge balance. The most dominant anion is sulfate. Ammonium is known to bond preferentially with sulfate in the reaction below (Husar 2013):

$$\mathbf{2\ NH_3 + H_2SO_4 \rightarrow (NH_4)_2SO_4}$$

However, the sulfate concentration is lower than the ammonium at all sites, so it alone cannot be fully neutralizing $NH_4^+$. Ammonium tends to pair next with nitrate, which is the second most abundant anion (IPCC 2007).

$$\mathbf{HNO_3 + NH_3 \rightarrow NH_4NO_3}$$

We initially expected that these two reactions would fully neutralize the ammonium and balance the charges of the aerosols in this size range, as the concentrations of the ions seemed to be balanced. Figure 11 shows the ammonium speciations. While the majority of $NH_4^+$ is indeed present as ammonium sulfate or ammonium nitrate (Lyons Spring has much higher concentrations of ammonium nitrate because of the abundance of aerosol nitrate - see page 25), there still remains some unpaired ammonium for the majority of the 48-hour intervals. Thus, even considering the large standard deviations, there must be an unidentified anion bonding with the ammonium.

To resolve this discrepancy, we returned to the ion chromatograms and found an additional peak that was determined to be oxalate ($C_2O_4^{2-}$). Oxalate can also neutralize ammonium, as shown in the following equation, so we included it in the ammonium speciation (Lefer &Talbot 2001; Figure 12).

$$\mathbf{2\ NH_3 + H_2C_2O_4 \rightarrow (NH_4)_2C_2O_4}$$

The addition of oxalate as a neutralizing agent was enough to fully neutralize the ammonium for some of the intervals, but many still had excess ammonium. The percent of ammonium that was present as ammonium oxalate (calculated by dividing the concentration of $(NH_4)_2C_2O_4$ by the concentration of $NH_4^+$) varied with each data set: the average percentage for concentration Lyons Spring, Lyons Summer, and Main Summer are 1.00% (standard deviation of 1.31%), 3.65% (standard deviation of 2.92%), and 4.33% (standard deviation of 3.95%), respectively. The number of completely explained days remained unchanged for Lyons Spring, probably because there was more nitrate to neutralize the ammonium, so oxalate was less impactful. However, these fully neutralized days increased from 3 to 9 for Lyons Summer, and from 4 to 5 days for Main Summer. The inclusion of the oxalate clearly had some impact, but there were still 31 time periods that had excess ammonium. This indicates that there is another anion that is pairing with the ammonium - likely an organic acid due to their prevalence in the fine mode - but we have yet to identify it. However, the role of oxalate in charge neutralization highlights its importance and abundance in the atmosphere and emphasizes the need to further understand its sources and formation mechanisms. Fortunately, the size and resolution of this data set offered a chance to look further into oxalate production pathways and to contribute to the general understanding of water-soluble organic compounds.

**Figure 10**: Average size distributions for a) Lyons Spring, b) Lyons Summer, and c) Main Summer.

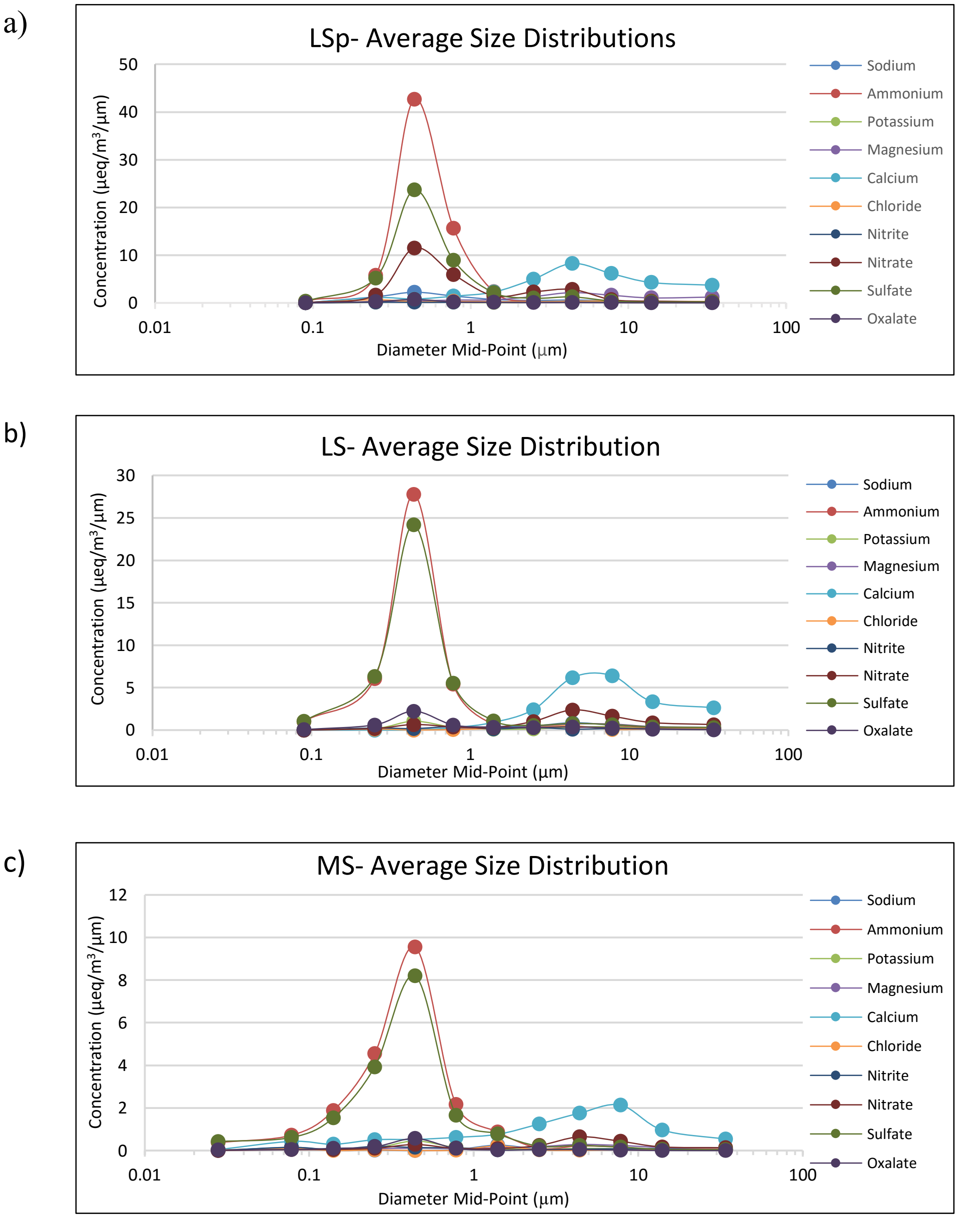

**Figure 11**: The ammonium speciation for a) Lyons Spring, b) Lyons Summer, and c) Main Summer. These graphs show that not all of the ammonium is neutralized by sulfate and nitrate.

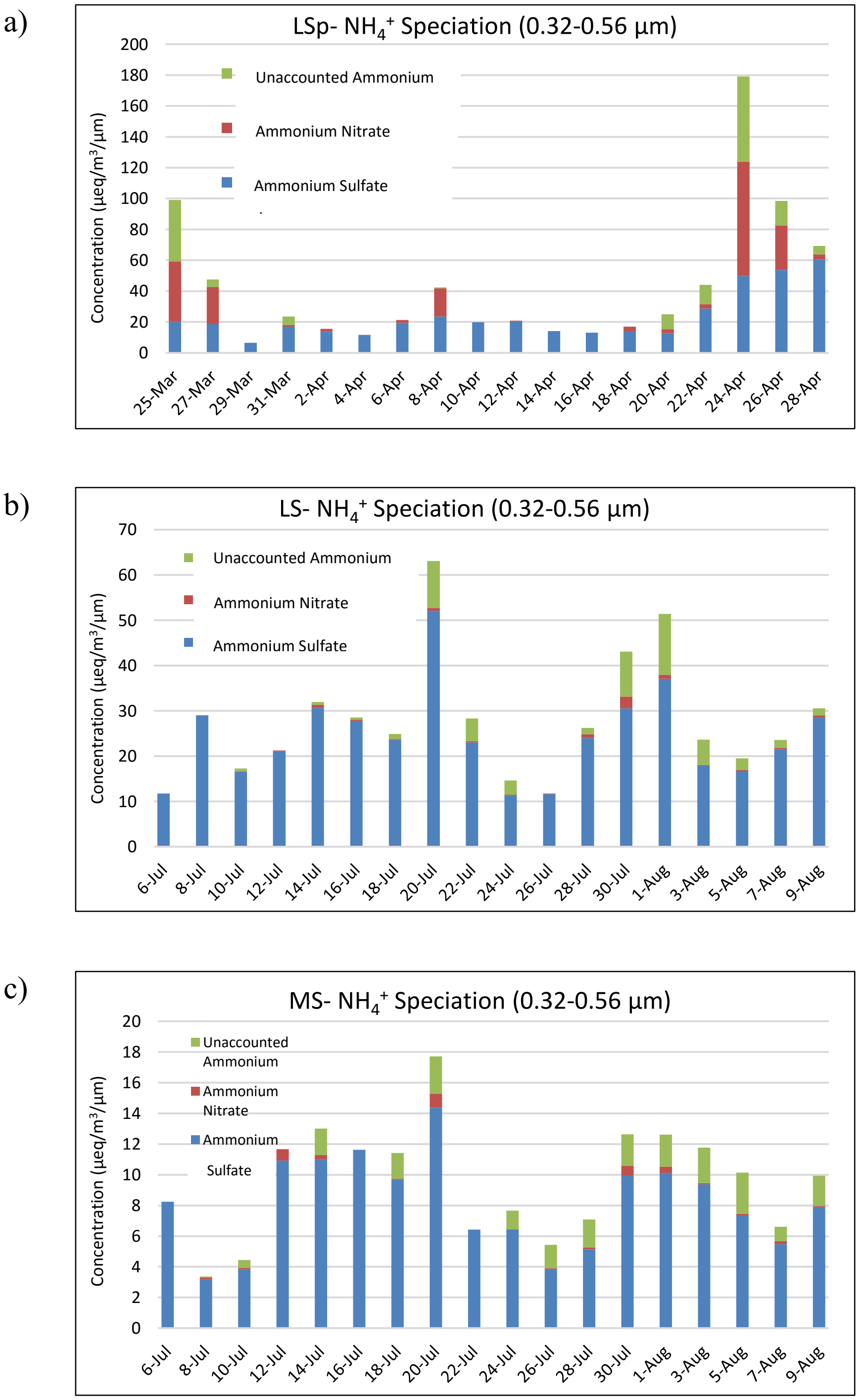

**Figure 12**: Ammonium speciation with oxalate included for a) Lyons Spring, b) Lyons Summer, and c) Main Summer. We find that $C_2O_4^{2-}$, $NO_3^-$, and $SO_4^{2-}$ are still not sufficient to completely neutralize $NH_4^+$.

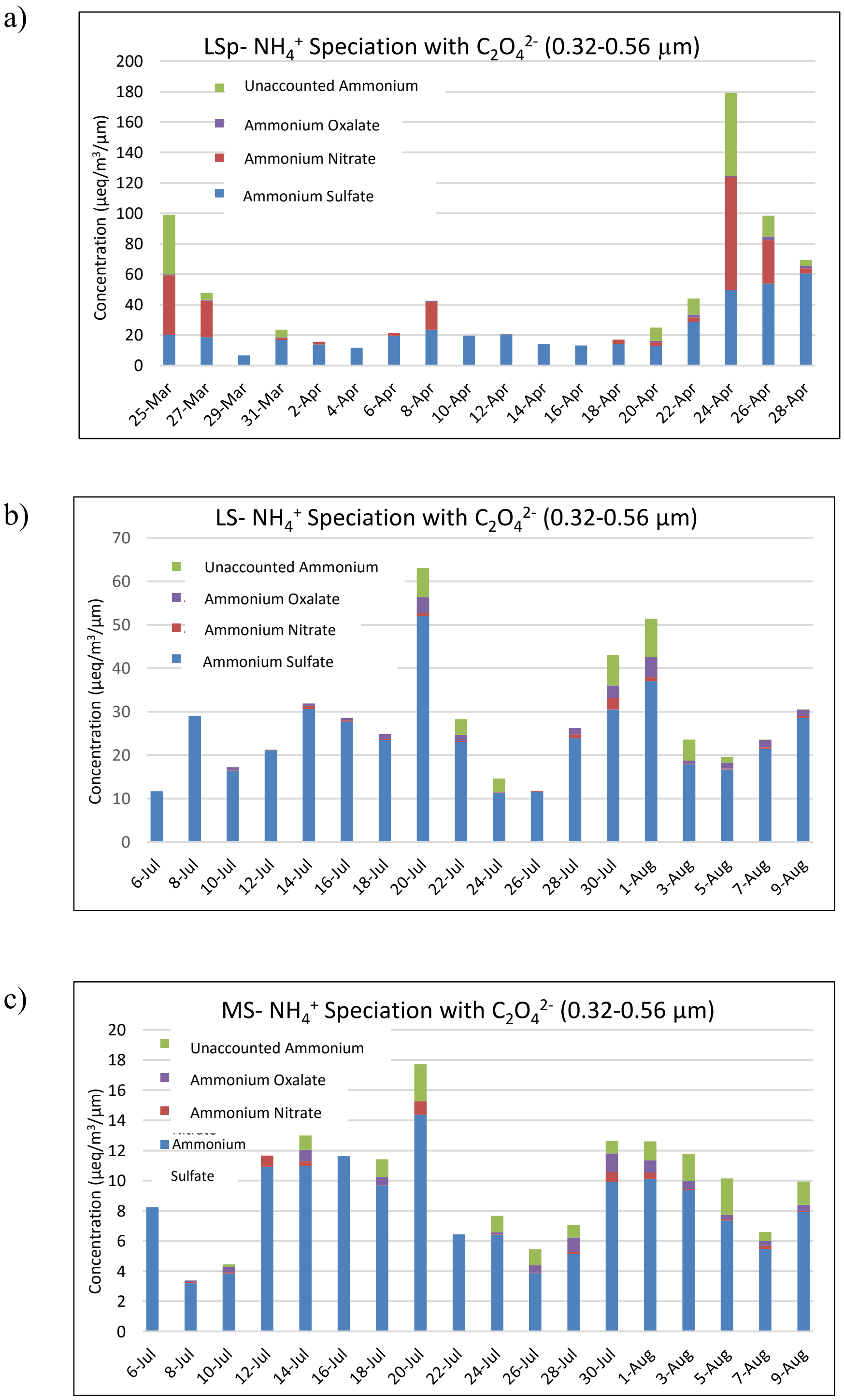

## Oxalate Sources and Formation Pathways

### *Biomass Burning*

Biomass burning (BB) is the combustion of organic material, either from natural or human-induced fires. This type of incomplete combustion has received attention for its contribution to the global carbon budget through both gaseous and aerosol emissions, its direct human health impacts, and its creation of haze (Cheng et al. 2013). It has been suggested that BB is a source of primary aerosol oxalate emission (Cheng et al. 2013). In places where biomass burning is a frequent occurrence, the resulting oxalate emissions might have notable effects on haze and aerosol properties (Jiang et al. 2011).

In order to understand the contribution of biomass burning to the overall concentrations of aerosol oxalate, we needed an indicator of burning in our data. Cheng et al. (2013) found that potassium is an acceptable indicator of BB, as it is present in organic matter and correlates with levoglucosan, the main product of the combustion of cellulose. Several other studies have used correlations between potassium and oxalate to determine the relative contributions of BB to total aerosol oxalate concentrations (Zhou et al., 2015; Jiang et al., 2011), so a similar method was applies to the dataset here.

These studies correlated the two species at a $PM_{2.5}$ size range, so our concentrations were estimated using the procedure outlined in the methods. The correlations yielded $r^2$ values of 0.354, 0.556, and 0.523 with statistically significant p-values << 0.01 for Lyons Spring, Lyons Summer, and Main Summer, respectively (Figure 13).

These moderate correlations between oxalate and potassium suggest that biomass burning is a notable contributor to oxalate concentrations. The correlations are much higher in the summer than in Lyons Spring. This is consistent with the satellite data suggesting that the majority of biomass burning in the United States between 2003 and 2007 occurred in July and August, supporting the idea that BB is an important direct source of aerosol oxalate (Zhang et al., 2009).

However, because of the high ratio of oxalate to potassium, it has been suggested that BB can be more than just a *direct* source of oxalate (Jiang et al., 2011). It is likely that oxalate precursors are being released, which form aerosol oxalate through secondary pathways (Jiang et al., 2011). It has not yet been determined which of the proposed secondary formation mechanisms is dominant: heterogeneous in-cloud oxidation or homogenous gas-state photochemical oxidation. The following sections will examine the two pathways through the lens of our data in order to see if one pathway seems to be dominant.

**Figure 13**: Correlations between aerosol $K^+$ and $C_2O_4^{2-}$ for a) Lyons Spring, b) Lyons Summer, and c) Main Summer.

a)

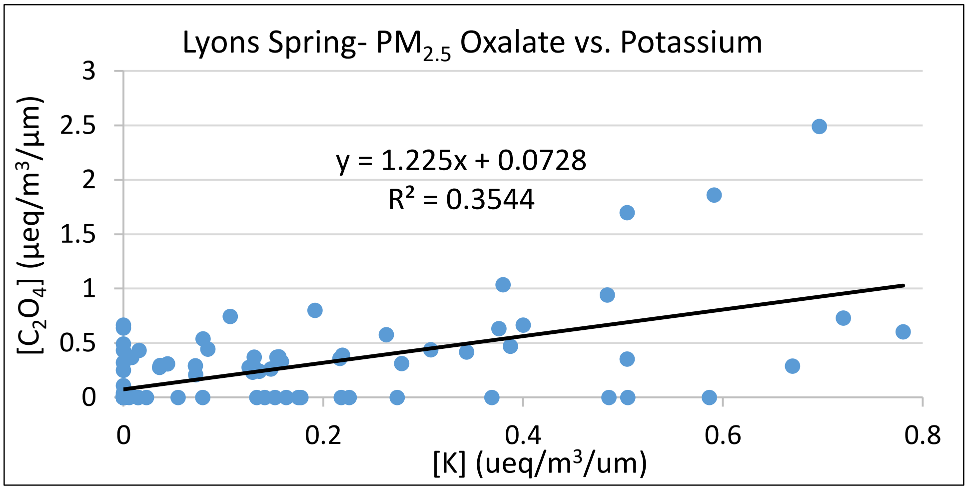

b)

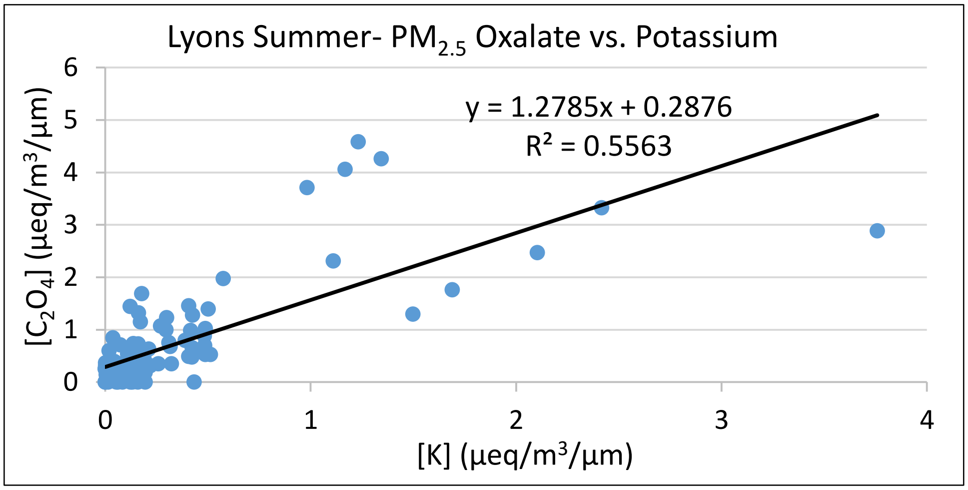

c)

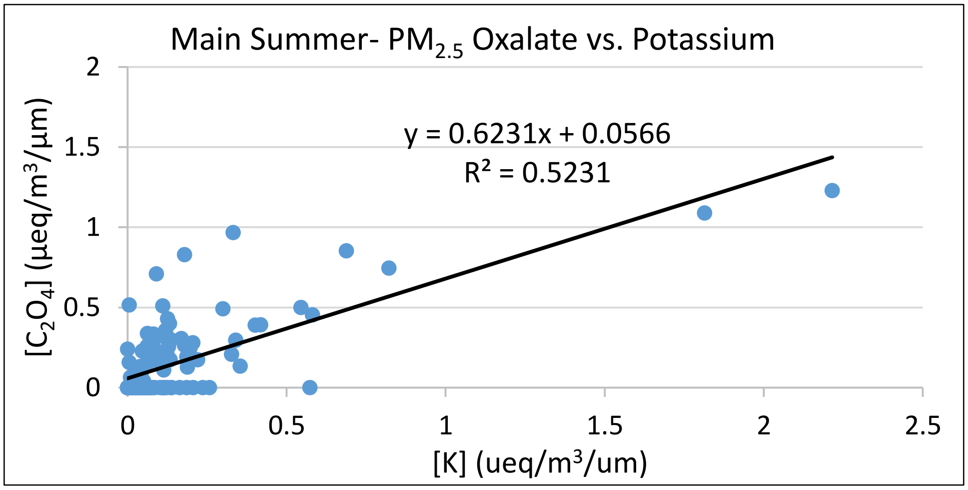

### *In-Cloud Processes*

The first proposed secondary formation mechanism for oxalate is in-cloud processes. This idea was originally suggested by Yu et al. (2005). The basis for this theory is the strong correlation between sulfate and oxalate, and the presence of both species in the droplet size range (Yu et al. 2005). The aqueous formation mechanism for sulfate is well established and accounts for the majority of aerosol sulfate formation (Seinfeld & Pandis 1998, Liao et al. 2003). It is supported by the large concentrations of sulfate in and above clouds relative to the smaller amounts below clouds. Yu (2005) ran correlations between the two species in the $PM_{2.5}$ range for 13 sites throughout eastern Asia using a multitude of methods over various time periods, and extracted similar correlations from past studies with comparable data. The $r^2$ values they found ranged between 0.49 and 0.95, suggesting a strong connection between oxalate and sulfate (Yu et al. 2005).

$PM_{2.5}$ concentrations of the ions were estimated as reported above. Because the peak concentrations of both species were in the 0.32-0.56 μm range, this captured the majority of the particles. Correlations between sulfate and oxalate for the different sites and seasons (Figure 14) indicated $r^2$ values for Lyons Spring, Lyons Summer, and Main Summer were 0.691, 0.788, and 0.512, respectively, all with p-values<0.001. All of these coefficients of determination are significant and within the range of those found by Yu et al. (2005), which appears to confirm the hypothesis that sulfate and oxalate both have in-cloud processing as the same dominant secondary formation pathway. The slightly lower correlation in the Main Summer data set might be explained by the less successful storage technique, resulting in aerosol losses in multiple samples and potentially contaminated blanks. Due to these factors, many of the oxalate levels for this set were below the Method Detection Limit of $2.87 \times 10^{-4}$ μeq/$m^3$/ μm. Despite this, the correlation was still moderately high at 0.513, lending further support to the in-cloud hypothesis.

The slopes of the regressions of oxalate vs. sulfate for Lyons Spring, Lyons Summer, and Main Summer are 0.028 (± 0.0036), 0.0875 (±0.0087), and 0.0573 (±0.0093), respectively. These are mostly within the range of Yu et al.'s (2005) slopes (between 0.0038 and 0.079). These slopes indicate the relative concentrations of oxalate to sulfate (or the ratio of their precursors), but not the absolute concentrations of the species or a potential shared formation pathway. Lyons Summer has the highest slope, indicating that there is more oxalate relative to sulfate than in the other data sets. Lyons Spring is the lowest, showing that there is more sulfate relative to oxalate. This is consistent with the expected emissions of $SO_2$, the primary precursor for sulfate. $SO_2$ is released when coal is combusted for heating purposes (Yu et al. 2005). It is far colder in the spring in Colorado than in the summer, so more $SO_2$ might be released for heating than in the summer. However, coal combustion for electricity generation for air conditioning might be significant in the warmer summer season. It is hard to say which process releases more cumulative sulfate, but the higher spring concentrations point to more coal burning for heating.

Another strong correlation that offers a competing formation pathway for oxalate is that between oxalate and ammonium. The $r^2$ values for this correlation Lyons Spring, Lyons Summer, and Main Summer are 0.464, 0.751, and 0.239, respectively, with p-values<0.001, (Figure 15). Because these correlations are relatively strong, and because, like sulfate and oxalate, both species peak in the 0.32-0.56 μm size range, it might be inferred that oxalate and ammonium have a common formation pathway. However, sulfate and ammonium concentrations are known to track each other, as ammonium is mainly produced in a reaction between gaseous nitric acid and aerosol sulfate. Therefore, the correlation between ammonium and oxalate is likely due to that relationship rather than a common formation pathway between ammonium and oxalate (Yu et al. 2005). This secondary connection between the two species is supported by the higher correlations of oxalate with sulfate than with ammonium. This relationship could also be an indicator that oxalate exists as aerosol ammonium oxalate, which does not point to any specific formation method but validates our reasons for exploring oxalate (Jiang et al. 2011).

**Figure 14**: Correlations between aerosol $SO_4^{2-}$ and $C_2O_4^{2-}$ for a) Lyons Spring, b) Lyons Summer, and c) Main Summer. The high correlations indicate a common secondary formation pathway.

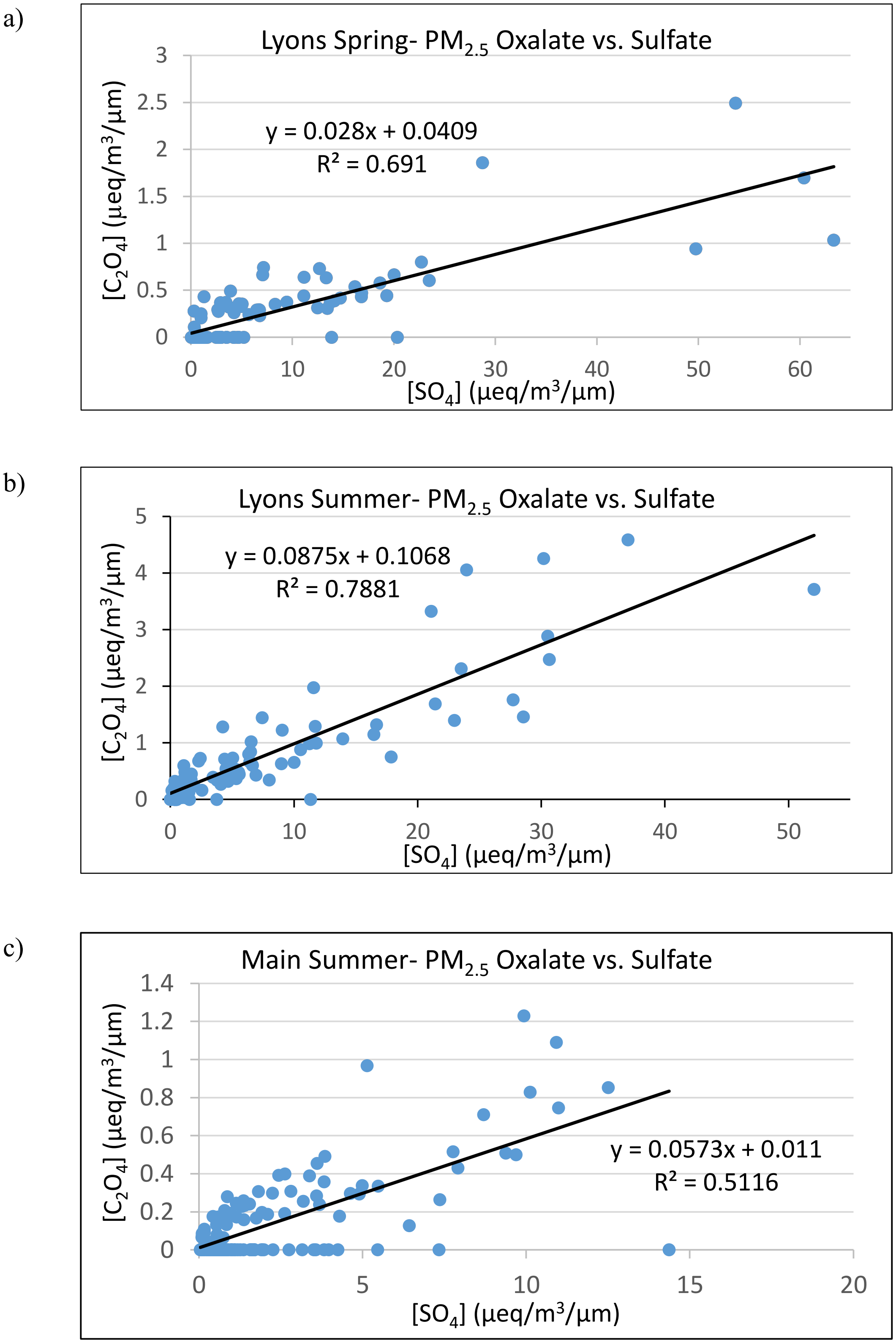

**Figure 15**: Correlations between aerosol $NH_4^+$ and $C_2O_4^{2-}$ for a) Lyons Spring, b) Lyons Summer, and c) Main Summer.

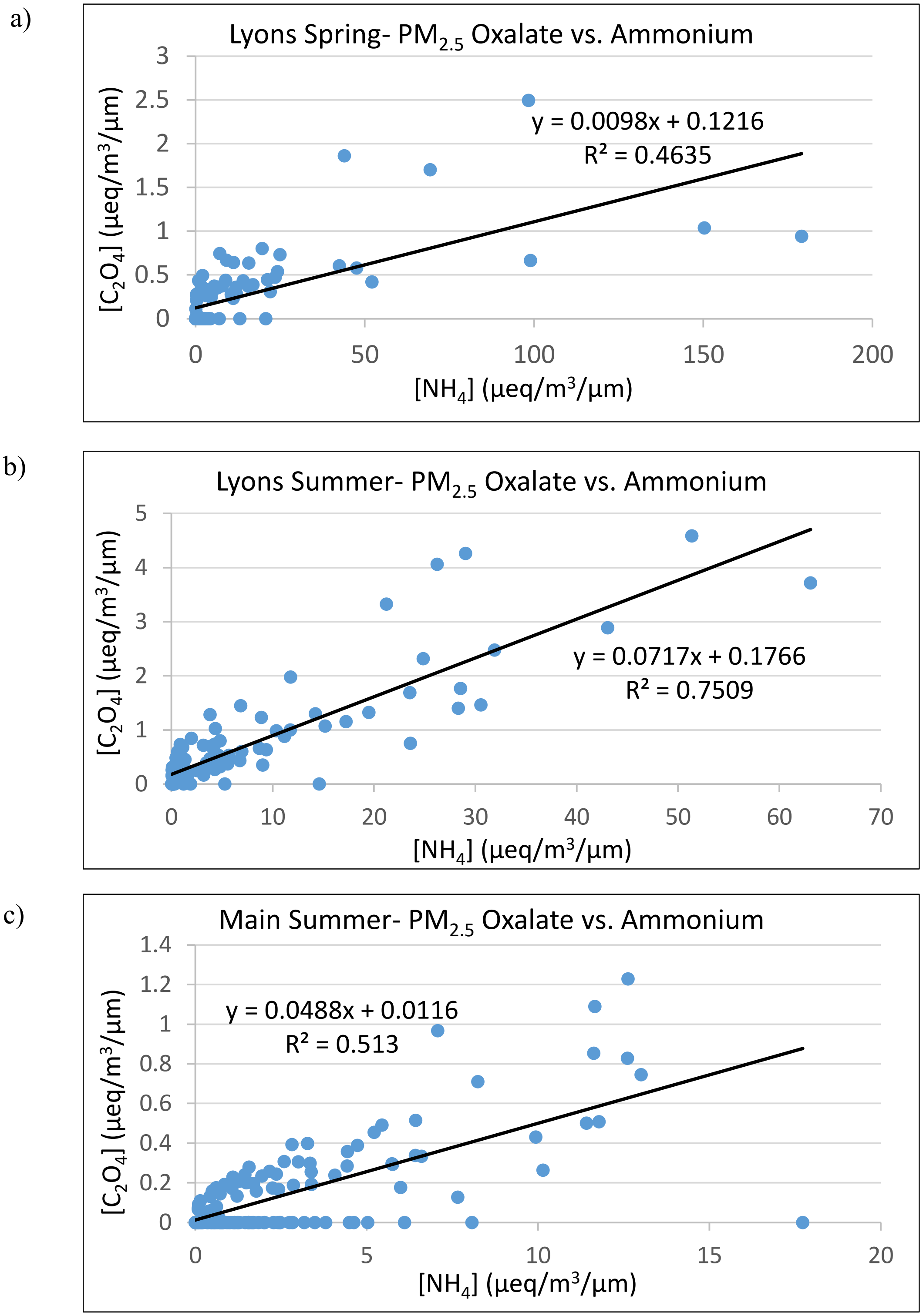

### *Gas-Phase Oxidation*

The second proposed mechanism is the traditionally assumed pathway for aerosol oxalate production: homogenous gas-phase photo-oxidation. In this scenario, oxalic acid is oxidized by a radical, likely OH, and then condensed into an aerosol.

The importance of this pathway is harder to prove with only aerosol data, as much of the evidence would need to be obtained from the gaseous chemistry. Other studies have estimated its relevance by correlating aerosol oxalate concentrations with the sum of gas-phase nitrogen dioxide and ozone, which are indicators of the homogenous secondary formation of nitrate (Zhou et al. 2015; Martinelango et al. 2007). Zhou et al. (2015) also used PMF to estimate the relative contributions of oxalate sources, and found that 33% could be attributed to homogenous mechanisms. Both Zhou et al. (2015) and Martinelango et al. (2007) collected highly time-resolved samples (to the hour), and were able to show a diurnal variation of oxalate concentration that was consistent with gas-phase photo-oxidation. However, the dataset for the present study lacks the time resolution and gas-phase data necessary to replicate these methods. Jiang et al. (2011) circumvented this problem by correlating aerosol nitrate with oxalate. While nitrate alone probably does not fully represent a homogenous reaction, Jiang et al. (2011) reasoned that a moderate or strong correlation might indicate a common formation pathway, as their formation would be dependent on the availability of the hydroxyl radical and thus linked.

Following this approach, nitrate and oxalate were correlated in the $PM_{2.5}$ size range. Jiang et al. (2011) did not report their $r^2$ values, so we could not compare our results to theirs; however, the $r^2$ values for Lyons Spring, Lyons Summer, and Main

Summer were 0.234, 0.271, and 0.280, respectively, all with p-values<0.001 (Figure 16). While these correlations are not particularly strong, they may still indicate that there is a connection between the two species. If gas-phase data were available for these sites and dates, the oxalate to nitrogen dioxide and ozone might be able to be compared for a more concrete conclusion. However, recall that in Lyons Spring there is more nitrate in the aerosol phase than in there is in the summer season (because of the lower temperatures). Therefore, the low correlation between aerosol nitrate and oxalate in this case might more strongly indicate that a homogenous pathway is not important in this season. Even for that data set, though, there is likely a considerable amount of nitrate in the gas-phase, so it does not preclude this mechanism. So, even with only the aerosol nitrate correlations, it can reasonably be assumed that gas-phase photo-oxidation is one of the secondary formation mechanisms for oxalate. However, it is not possible to determine the relative contribution of in-cloud and gas-phase processes with only this information.

**Figure 16**: Correlations between aerosol $NO_3^-$ and $C_2O_4^{2-}$ for a) Lyons Spring, b) Lyons Summer, and c) Main Summer.

a)

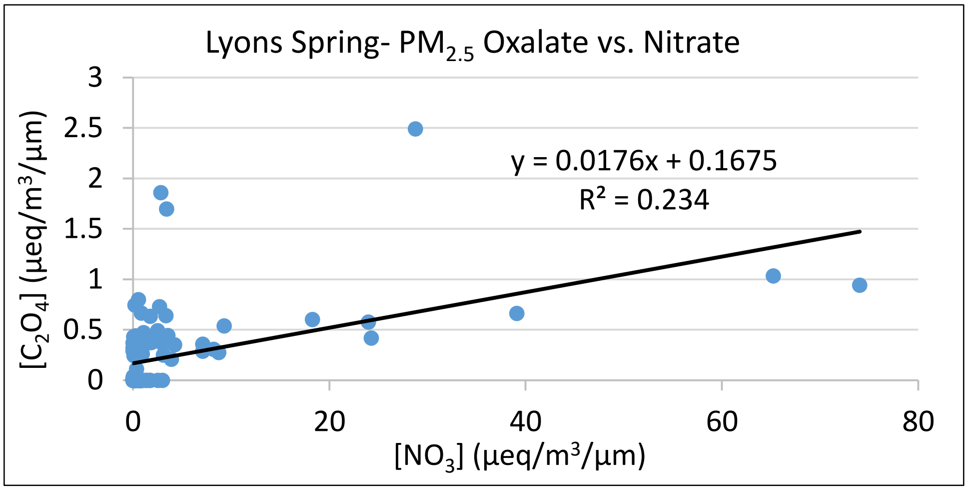

b)

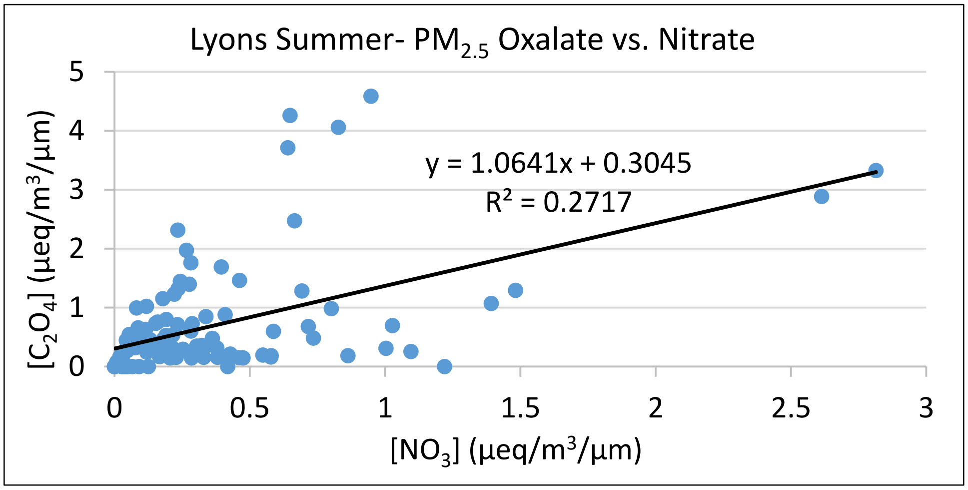

c)

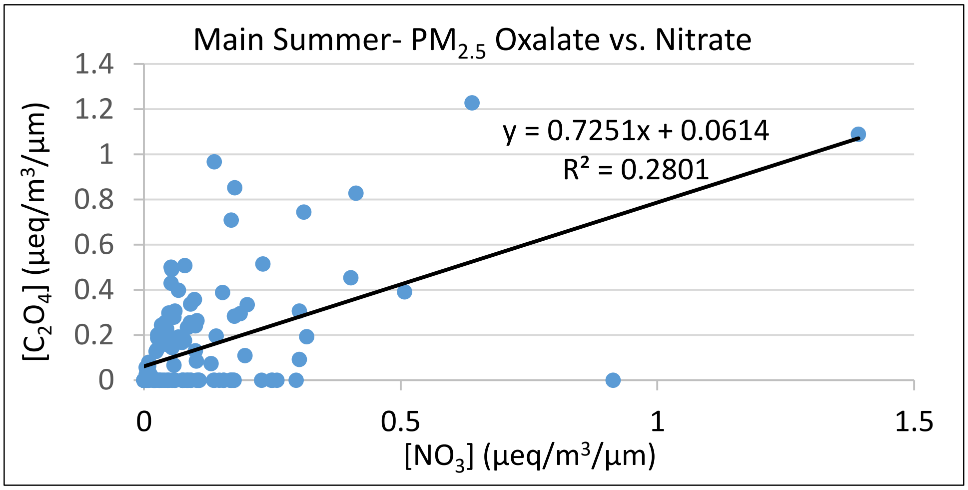

## Conclusions

Rocky Mountain National Park is an incredibly beautiful and valuable ecosystem that deserves to be preserved. Gathering knowledge about aerosol pollutants that are impactful to the park is important in implementing policies that alleviate potential harm from these particles. More than that, however, our rapidly changing climate and prevalent haze has incited a need to better understand factors that impact the planet's radiative balance and hinder visibility, such as aerosols. WSOCs have been particularly neglected in this pursuit, although they are a major and sometimes dominant component of aerosol composition. Little is known about the sources and formation pathways of many WSOCs, which prevents the creation of appropriate mitigation techniques. Because of its relative abundance and chemical simplicity, oxalate can serve as representative for WSOCs. This study contributes to the debate about oxalate secondary formation mechanisms, allowing scientists and policy makers to craft better-informed models and policies.

The goal of this study, and of the larger RoMANS study, was to learn more about the composition and size distribution of aerosols in and around RMNP, so that the sources and formation mechanisms of important species could be identified and addressed. The dominant cation in the fine mode was ammonium, and the dominant anions were sulfate (by far the most abundant at all sites on all days), nitrate, and oxalate. All of these species peaked in the 0.32-0.56 μm size range, except for nitrate in the summer season. Under the hotter summer temperatures, more nitrate was present in the gas phase, which was not measured. Therefore, the nitrate in this season was primarily present in the coarse mode, between 3.2 and 5.6 μm. The Lyons Spring nitrate also had a notable peak in this range, despite larger amounts of fine aerosol. This coarse-mode nitrate is the result of a reaction with coarse calcium carbonate from dust and has significant impacts on RMNP's sensitive ecosystems. Studies such as Beem et al. (2010) and Benedict et al. (2013) have likewise noticed these high concentrations of coarse-mode nitrate and detailed the distribution and sources of the species. The combination of sulfate, nitrate, and oxalate in the 0.32-0.56 μm size range neutralized the majority of the ammonium in the same size bin, but the remaining ammonium in almost every 48-hour period indicated that unidentified organic acids are significant in the neutralization process.

Aerosol oxalate became the focus of the study, as its relative abundance in the atmosphere and its role as a proxy for other WSOCs has become increasingly apparent and therefore important to aerosol chemistry. We found that oxalate, like the other major compounds, is dominant in the 0.32-0.56 μm size range. This allows it to act as a neutralizing agent for ammonium. We attempted to determine the sources and secondary formation pathways of oxalate by correlating it with indicator species. Oxalate was moderately correlated with potassium ($r^2$ values between 0.354 and 0.556), which is a tracer for biomass burning. It was also somewhat correlated with nitrate ($r^2$ values between 0.234 and 0.280), indicating that gas-phase photo-oxidation is a potential secondary formation pathway. However, the lack of gas-phase nitrogen dioxide and ozone data (both of which are involved in photochemical pathways) prevented a more confident assessment of the importance of this mechanism. The strong correlation between sulfate, which is almost completely formed through in-cloud processes, and oxalate ($r^2$ values between 0.512 and 0.788) supported Yu et al.'s (2005) hypothesis that this pathway is a major contributor to fine-mode oxalate concentrations. All three mechanisms are supported by the data and are likely occurring in RMNP; however, the relative contributions of each remains unclear at this point. Due to the number of local conditions that impact these pathways (agricultural burning and wildfires, solar radiation, and precipitation), there is a lack of consensus between studies about their relative importance, though most do agree that all three play a role (Yu et al. 2005, Jiang et al. 2007, Martinelango et al. 2007, Zhou et al. 2015).

There were a number of additional components that would have allowed this study to draw more concrete conclusions and contribute further to the field. Firstly, the Main Spring samples would have allowed us to conduct a more detailed seasonal comparison between the Main and Lyons sites. With both seasons at both sites, we could have clearly attributed variation between data sets to differences in season and location. However, with the available data it was still possible to identify obvious and important differences along the two variables.

The MOUDI data collected by the RoMANS team for this study was both expansive and in-depth. Much of the ambiguity in these conclusions stemmed from a lack (or lack of ability to find) other types of data that would have supported specific oxalate sources and secondary formation pathways. With access to gas-phase nitrogen dioxide and ozone data, which are associated with gas-phase photo-oxidation, we could better determine the importance of this pathway in oxalate formation. Correlating oxalate concentrations with relative humidity and precipitation or with solar radiation might have pointed towards gas-phase or in-cloud processing as the dominant secondary mechanism. Records of these types of data might exist, but perhaps due to the long wait between sample collection and analysis (almost ten years) they were difficult to find.

This study provides many opportunities for future research. Applying a factor analysis model such as Positive Matrix Factorization (PMF) and gathering more information on tracer and indicator species would allow more effective profiles to determine the relative contributions of oxalate emission and formation sources. Although the results of other studies indicate that this is site-specific, having a broader selection of locations and relative contributions can help identify the most influential factors in determining the dominant mechanism. It would also be useful to run higher resolution HYSPLIT back-trajectories that capture the variation in elevation between the two sites and better account for local circulation patterns. By comparing these back-trajectories to days with high aerosol concentrations, we could perhaps identify the sources of key emissions and precursors.

Further research is also needed to specify the overall WSOC concentrations and composition. Broadening our knowledge about the other types of organics in RMNP, which seem plentiful based on our failure to completely neutralize the ammonium, would increase our ability to account for the effects of aerosols on climate and visibility. Organics are clearly an important component of the atmosphere and their impacts need further research so that they can be effectively addressed by policy decisions.

## Acknowledgments

I would like to thank the many people were involved in the creation and execution of this thesis. My first debt of gratitude goes to Howard Drossman. Howard has been my guide, my advocate, and my mentor throughout my college career. He was the first to inspire my love for environmental science and he convinced me that I could succeed in the sciences. He nominated me for the Center for Multiscale Modeling of Atmospheric Sciences (CMMAP) REU internship for the summer of 2015, which provided the research around which this thesis is based.

Next, I want to thank Lynne Gratz, who took me on as her first thesis student, despite never having met or taught me. She worked patiently with me, revising and editing multiple drafts of my thesis and providing great insight into the field of atmospheric science. If there was component of the thesis process with which she was unfamiliar, she went out of her way to get that knowledge. Lynne's patience and willingness to help made this work possible.

My next thanks goes to Katie Benedict and Jeff Collett, my mentors at CSU. Jeff extended his group's resources and personnel, as well as his own valuable time and guidance throughout my time at CMMAP. Katie was always there to help me with day-to-day operations. She was unfailingly patient and supportive while I daily broke the IC and struggled my way through data analysis. On that note, I would like to thank the entire atmospheric chemistry team, who helped me with my lab work and fixed my many mistakes. I learned so much from everyone at CSU, and I am so grateful for all of their help.

My final thanks (though there are many more who deserve my gratitude) is for the CMMAP program, and everyone involved in this incredible REU. Melissa Burt was always there to make me laugh and provide me with great conversation. I could not have asked for a better group of fellow CMMAP interns. They made my summer in Fort Collins one of the best in my life, and I hope to remain as close with them in years to come as we still are today. This work has been supported by the National Science Foundation Science and Technology Center for Multi-Scale Modeling of Atmospheric Processes, managed by Colorado State University under cooperative agreement No. ATM-042524.

# References

Allen, H. M., Draper, D. C., Ayres, B. R., Ault, A., Bondy, A., Takahama, S., ... & Laskin, A. (2015). Influence of crustal dust and sea spray supermicron particle concentrations and acidity on inorganic NO 3− aerosol during the 2013 Southern Oxidant and Aerosol Study. *Atmospheric Chemistry and Physics*, *15*(18), 10669-10685.

Beem, K. B., Raja, S., Schwandner, F. M., Taylor, C., Lee, T., Sullivan, A. P., ... & Hand, J. (2010). Deposition of reactive nitrogen during the Rocky Mountain Airborne Nitrogen and Sulfur (RoMANS) study. *Environmental Pollution*, *158*(3), 862-872.

Benedict, K. B., Day, D., Schwandner, F. M., Kreidenweis, S. M., Schichtel, B., Malm, W. C., & Collett, J. L. (2013). Observations of atmospheric reactive nitrogen species in Rocky Mountain National Park and across northern Colorado. *Atmospheric Environment*, *64*, 66-76.

Change, C. (2007). The Physical Science Basis, Contribution of Working Group I to the Fourth Assessment Report of the Intergovernmental Panel on Climate Change, 2007, S. Solomon, D. Qin, M.

Cheng, Y., Engling, G., He, K. B., Duan, F. K., Ma, Y. L., Du, Z. Y., ... & Weber, R. J. (2013). Biomass burning contribution to Beijing aerosol. *Atmospheric Chemistry and Physics*, *13*(15), 7765-7781.

Cruz, C. N., & Pandis, S. N. (1997). A study of the ability of pure secondary organic aerosol to act as cloud condensation nuclei. *Atmospheric Environment*, *31*(15), 2205-2214.

Duan, J. C., Bi, X. H., Tan, J. H., Sheng, G. Y., & Fu, J. M. (2006). The particle diameter distribution of polycyclic aromatic hydrocarbons (PAHs) in atmospheric particle during haze period in Guangzhou. *China Environmental Science*, *26*(1), 6-10.

Ervens, B. T. B. W. R., Turpin, B. J., & Weber, R. J. (2011). Secondary organic aerosol formation in cloud droplets and aqueous particles (aqSOA): a review of laboratory, field and model studies. *Atmospheric Chemistry and Physics*, *11*(21), 11069-11102.

Hänel, G. (1976). The properties of atmospheric aerosol particles as functions of the relative humidity at thermodynamic equilibrium with the surrounding moist air. *Adv. Geophys*, *19*(1), 73-188.

Huang, X. F., Yu, J. Z., He, L. Y., & Yuan, Z. (2006). Water‐soluble organic carbon and oxalate in aerosols at a coastal urban site in China: Size distribution characteristics, sources, and formation mechanisms. *Journal of Geophysical Research: Atmospheres (1984–2012)*, *111*(D22).

Husar, R. B., Lodge, J. P., & Moore, D. J. (Eds.). (2013). *Sulfur in the Atmosphere: Proceedings of the International Symposium Held in Dubrovnik, Yugoslavia, 7-14 September 1977* (Vol. 12, No. 1-3). Elsevier.

Jiang, Y., Zhuang, G., Wang, Q., Liu, T., Huang, K., Fu, J. S., ... & Deng, C. (2011). Characteristics, sources and formation of aerosol oxalate in an Eastern Asia megacity and its implication to haze pollution. *Atmospheric Chemistry and Physics Discussions*, *11*(8), 22075-22112.

Kalberer, M., Yu, J., Cocker, D. R., Flagan, R. C., & Seinfeld, J. H. (2000). Aerosol formation in the cyclohexene-ozone system. *Environmental Science & Technology*, *34*(23), 4894-4901.

Kanakidou, M., Seinfeld, J. H., Pandis, S. N., Barnes, I., Dentener, F. J., Facchini, M. C., ... & Swietlicki, E. (2005). Organic aerosol and global climate modelling: a review. *Atmospheric Chemistry and Physics*, *5*(4), 1053-1123.

Kaufman, Y. J., Tanré, D., & Boucher, O. (2002). A satellite view of aerosols in the climate system. *Nature*, *419*(6903), 215-223.

Kavouras, I. G., Mihalopoulos, N., & Stephanou, E. G. (1998). Formation of atmospheric particles from organic acids produced by forests. *Nature*, *395*(6703), 683-686.

Lee, T., Yu, X. Y., Ayres, B., Kreidenweis, S. M., Malm, W. C., & Collett, J. L. (2008). Observations of fine and coarse particle nitrate at several rural locations in the United States. *Atmospheric Environment*, *42*(11), 2720-2732.

Lefer, B. L., & Talbot, R. W. (2001). Summertime measurements of aerosol nitrate and ammonium at a northeastern US site. *Journal of Geophysical Research: Atmospheres (1984–2012)*, *106*(D17), 20365-20378.

Liao, H., Adams, P. J., Chung, S. H., Seinfeld, J. H., Mickley, L. J., & Jacob, D. J. (2003). Interactions between tropospheric chemistry and aerosols in a unified general circulation model. *Journal of Geophysical Research: Atmospheres (1984–2012)*, *108*(D1), AAC-1.

Lipsey, Mark W. & Wilson, D. B. (2001). *Practical meta-analysis* (Vol. 49). Thousand Oaks, CA: Sage publications.

Martinelango, P. K., Dasgupta, P. K., & Al-Horr, R. S. (2007). Atmospheric production of oxalic acid/oxalate and nitric acid/nitrate in the Tampa Bay airshed: Parallel pathways. *Atmospheric Environment*, *41*(20), 4258-4269.

Positive Matrix Factorization Model for environmental data analyses: What is the Positive Matrix Factorization Model?. (2015). *Environmental Protection Agency Web site*: Accessed March 26, 2016.

RoMANS: Rocky Mountain Atmospheric Nitrogen and Sulfur Study. (October 2009). *National Park Service Web site*: Accessed March 26, 2016.

Santos, L. C., Poli, A. L., Cavalheiro, C., & Neumann, M. G. (2009). The UV/H2O2-photodegradation of poly (ethyleneglycol) and model compounds. *Journal of the Brazilian Chemical Society*, *20*(8), 1467-1472.

Saxena, P., Hildemann, L. M., McMurry, P. H., & Seinfeld, J. H. (1995). Organics alter hygroscopic behavior of atmospheric particles. *Journal of Geophysical Research: Atmospheres* (1984–2012), 100(D9), 18755-18770.

Seinfeld, J. H., & Pandis, S. N. (2006). *Atmospheric Chemistry and Physics*. Academic Press: Hoboken.

Seinfeld, J. H., & Pandis, S. N. (2012). *Atmospheric Chemistry and Physics: from air pollution to climate change*. John Wiley & Sons.

Skoog, D. A., West, D. M., Holler, F. J. (1995). *Fundamentals of Analytical Chemistry* (7th ed.). Brooks/Cole Publishing Company: New York.

Stelson, A. W., & Seinfeld, J. H. (1982). Relative humidity and temperature dependence of the ammonium nitrate dissociation constant. *Atmospheric Environment (1967)*, *16*(5), 983-992.

Stocker, T. F., Qin, D., Plattner, G. K., Tignor, M., Allen, S. K., Boschung, J., ... & Midgley, B. M. (2013). IPCC, 2013: climate change 2013: the physical science basis. Contribution of working group I to the fifth assessment report of the intergovernmental panel on climate change.

Visibility: Basic information. (2015). *Environmental Protection Agency Web site*: Retrieved from http://www3.epa.gov/visibility/what.html

Wall, S. M., John, W., & Ondo, J. L. (1988). Measurement of aerosol size distributions for nitrate and major ionic species. *Atmospheric Environment (1967)*, *22*(8), 1649-1656.

Whitby, K. T., & Cantrell, B. (1976). Atmospheric aerosols- Characteristics and measurement. In *International Conference on Environmental Sensing and Assessment, Las Vegas, Nev* (p. 1).

Willeke, K., & Whitby, K. T. (1975). Atmospheric aerosols: size distribution interpretation. *Journal of the Air Pollution Control Association*, *25*(5), 529-534.

Yu, J. Z., Huang, X. F., Xu, J., & Hu, M. (2005). When aerosol sulfate goes up, so does oxalate: implication for the formation mechanisms of oxalate. *Environmental Science & Technology*, *39*(1), 128-133.

Zhang, X., Kondragunta, S., & Ruminski, M. (2009). Spatiotemporal variations In Burned Areas and Biomass Burning Emissions Derived from Multiple Satellite-Based Active Fires across the USA. In *18th Annual International Emission Inventory Conference" Comprehensive Inventories-Leveraging Technology and Resources", Baltimore, Maryland (papers and presentations)*.

Zhou, Y., Huang, X. H., Bian, Q., Griffith, S. M., Louie, P. K., & Yu, J. Z. (2015). Sources and atmospheric processes impacting oxalate at a suburban coastal site in Hong Kong: Insights inferred from 1 year hourly measurements. *Journal of Geophysical Research: Atmospheres*, *120*(18), 9772-9788.

Zhuang, H., Chan, C. K., Fang, M., & Wexler, A. S. (1999). Formation of nitrate and non-sea-salt sulfate on coarse particles. *Atmospheric Environment*, *33*(26), 4223-4233.